Communications on Applied Mathematics and Computation (2022) 4:530–562
https://doi.org/10.1007/s42967-021-00127-4

ORIGINAL PAPER

Arbitrary Lagrangian-Eulerian Discontinuous Galerkin Methods for KdV Type Equations

Xue Hong[1] · Yinhua Xia[1]

Received: 22 August 2020 / Revised: 3 January 2021 / Accepted: 27 February 2021 /
Published online: 7 July 2021

Abstract
In this paper, several arbitrary Lagrangian-Eulerian discontinuous Galerkin (ALE-DG) methods are presented for Korteweg-de Vries (KdV) type equations on moving meshes. Based on the L^2 conservation law of KdV equations, we adopt the conservative and dissipative numerical fluxes for the nonlinear convection and linear dispersive terms, respectively. Thus, one conservative and three dissipative ALE-DG schemes are proposed for the equations. The invariant preserving property for the conservative scheme and the corresponding dissipative properties for the other three dissipative schemes are all presented and proved in this paper. In addition, the L^2 -norm error estimates are also proved for two schemes, whose numerical fluxes for the linear dispersive term are both dissipative type. More precisely, when choosing the approximation space with the piecewise kth degree polynomials, the error estimate provides the kth order of convergence rate in L^2-norm for the scheme with the conservative numerical fluxes applied for the nonlinear convection term. Furthermore, the $(k+1/2)$th order of accuracy can be proved for the ALE-DG scheme with dissipative numerical fluxes applied for the convection term. Moreover, a Hamiltonian conservative ALE-DG scheme is also presented based on the conservation of the Hamiltonian for KdV equations. Numerical examples are shown to demonstrate the accuracy and capability of the moving mesh ALE-DG methods and compare with stationary DG methods.

Keywords Arbitrary Lagrangian-Eulerian discontinuous Galerkin methods · KdV equations · Conservative schemes · Dissipative schemes · Error estimates

Mathematics Subject Classification 65M60 · 65M12

1 Introduction

We are concerned with solving the following KdV type equation:

✉ Yinhua Xia
yhxia@ustc.edu.cn

Xue Hong
xuehong1@mail.ustc.edu.cn

[1] School of Mathematical Sciences, University of Science and Technology of China, Hefei 230026, Anhui, China

$$\begin{cases} u_t + (f(u))_x + u_{xxx} = 0, (x, t) \in \Omega \times (0, T), \\ u(x, 0) = u_0(x), \quad x \in \Omega \end{cases} \tag{1}$$

with the periodic or other proper boundary conditions when Ω is a finite domain. The KdV equation may also be an initial value problem, which is defined in the whole domain with the initial condition only. Numerically, one of the commonly used strategies is to solve the infinite domain with periodic or compactly supported boundary conditions, if the initial condition decays fast in space. The KdV equation is a mathematical model of the wave propagation and can be applied to many fields, such as the oceanography, aeronautics, geology, plasma physics and many others. Boussinesq (1877) first introduced the KdV equation and Korteweg et al. in 1895 [26] rediscovered it, and in their study of the water wave, two classic solutions of the cnoidal wave and the solitary wave are discussed.

Many numerical methods were used to solve KdV equations, including pseudo-spectral methods by Fornberg et al. [12], finite difference schemes [15, 33], the heat balance integral method [27], the finite element method, and specially the discontinuous Galerkin (DG) method. The DG method is a class of finite element methods and its approximation space consists of completely discontinuous piecewise polynomials, which leads to the advantages of parallel efficiency, shock capturing and high-order accuracy etc. Reed et al. [30] firstly constructed the DG scheme for the neutron transport equation. Subsequently, Cockburn et al. developed the Runge-Kutta discontinuous Galerkin (RKDG) method for the nonlinear hyperbolic conservation laws in [5–8] and also proved its high order accuracy in [4, 9]. The key of this method is to design suitable numerical fluxes in order to make the scheme stable and high order accurate in various situations. For certain conserved energy, the conservative or dissipative fluxes are adopted to ensure the energy conservation or stability of the scheme. In the numerical experiments of [2, 41], the higher accuracy and better stability of the conservative scheme over long temporal intervals can be seen. Usually, we consider the conservation of the L^2 energy

$$E = \int \frac{u^2}{2} \mathrm{d}x.$$

The conservation of the Hamiltonian

$$H = \int \left(\frac{u_x^2}{2} - V(u) \right) \mathrm{d}x, \ V(u) = \int^u f(\xi) \mathrm{d}\xi \tag{2}$$

is also considered since the KdV equation is the Hamiltonian system [14]. Within the DG framework, the local discontinuous Galerkin (LDG) method was used to deal with derivatives of order higher than one. Yan et al. [38] developed an LDG numerical method for a general KdV type equation and proved the suboptimal convergence rate for linear wave KdV equations, and Xu et al. further designed the LDG method to solve a series of nonlinear wave equations [35, 36] and proved the suboptimal convergence rate. More recently, Xu et al. proved the optimal convergence rate for linear KdV equations in [37]. It is worth noting that the scheme is only for the dissipative scheme for both linear and nonlinear terms in terms of the energy E. The E conserved LDG and ultra-weak DG schemes were proposed in [2, 22, 41]. In addition, the Hamiltonian conserved LDG schemes were presented in [29, 41]. Usually, the conservative schemes can reduce the long-time phase error and improve the accuracy. Following the LDG method on static meshes for this problem, we are interested in solving KdV equations by the arbitrary Lagrangian-Eulerian discontinuous Galerkin (ALE-DG) method on adaptive moving meshes.

We can consider the ALE-DG method as a moving mesh DG method and its mesh motion follows the ALE method [11, 17], which allows the motion of the mesh to be like either the Lagrangian or the Eulerian description of motion. In recent years, Klingenberg et al. developed an ALE-DG method for conservation laws [13, 24] and Hamilton-Jacobi equations [25], where local affine linear mappings connecting the cells for the current and next time levels are defined and yield the time-dependent approximation space. Within very mild conditions on mesh movements, the stability and high order accuracy can be obtained for the method, where the mesh movement function is assumed to be piecewise linear [42]. They also showed that the ALE-DG method satisfies the geometric conservation law (GCL) for any Runge-Kutta scheme, which is significant for the ALE method and has been analyzed by Guillard et al. [16]. The ALE-DG method shares many good properties of the DG method defined on static grids, e.g., the entropy stability, the high order accuracy, the local maximum principle, and so on.

Since solutions of KdV equations often have the local structures, the mesh adaptation has been an important tool which focuses on the computational effort where it is most needed. In the ALE-DG method, we want to use the r-adaptive method without changing the number of mesh points and more grid points should be clustered in the area with wave to obtain better resolution comparing with the DG method on the static mesh. In recent years, a few research works are implemented in this aspect. Particularly, Tang et al. proposed the r-adaptive algorithm to the DG method for conservation laws in [10, 28, 32], in which they still need a conservative remapping projection from the new adaptive mesh to the last level mesh. Another motivation for designing the ALE-DG method is that KdV equations may contain the solitary wave solution (soliton), which is defined on the whole domain. One of the commonly used strategies is to solve the problem only in a finite domain with the periodic or compactly supported boundary conditions since the soliton decays very fast in space. But for long-time simulations, the computational domain should be large enough to justify this choice, thus it may not be very efficient. The ALE-DG method allows us to solve the equations in a moving computational domain and track the soliton waves.

In this work, we present the conservative and dissipative ALE-DG methods for this equation with the stability and error estimates. When adaptive meshes are adopted, the schemes can reduce the phase error efficiently comparing with the LDG method on static grids. Although many works have been done with adaptive mesh methods and DG methods, few works have combined adaptive mesh with DG methods to solve KdV equations in an appropriate way without the need of remapping. In the ALE-DG methods, after we get the mesh-redistribution at the next time level, the numerical solution will be evolved directly from the former time level to the next time level between two different meshes. We refer to Huang et al. [20] and Hong et al. [18] for the adaptive mesh generation.

The outline of this paper is as follows. In Sect. 2, we introduce the ALE-DG method for KdV equations and construct conservative and dissipative schemes, and also give their L^2 or Hamiltonian stability. Section 3 is devoted to the L^2 norm error estimates for two dissipative schemes of problem (1) with $f(u) = u^2$. Section 4 presents the methodology of adaptive moving meshes we use. In Sect. 5, some numerical results are demonstrated to validate the accuracy and effectiveness of the ALE-DG scheme. Finally, some conclusions are given in Sect. 6.

2 The ALE-DG Method

In this section, we develop the ALE-DG schemes based on either L^2 or Hamiltonian stability.

In order to describe the ALE-DG method, we need to take account of the motion of the grid for the time-dependent domain $\Omega(t)$. Given grid points $\left\{x^n_{j-\frac{1}{2}}\right\}_{j=1}^{N}$ at the time level t_n, so as $\left\{x^{n+1}_{j-\frac{1}{2}}\right\}_{j=1}^{N}$ at t_{n+1}, such that

$$\Omega(t^n) = \bigcup_{j=1}^{N}\left[x^n_{j-\frac{1}{2}}, x^n_{j+\frac{1}{2}}\right], \quad \text{and} \quad \Omega(t^{n+1}) = \bigcup_{j=1}^{N}\left[x^{n+1}_{j-\frac{1}{2}}, x^{n+1}_{j+\frac{1}{2}}\right]. \tag{3}$$

Assume that the first point and the last point could move at the same speed for the periodic boundary problem and stay the same for the fixed boundary problem. Next, we define

$$w_{j-\frac{1}{2}} := \frac{x^{n+1}_{j-\frac{1}{2}} - x^n_{j-\frac{1}{2}}}{t_{n+1} - t_n}, \quad x_{j-\frac{1}{2}}(t) = x^n_{j-\frac{1}{2}} + w_{j-\frac{1}{2}}(t - t_n) \tag{4}$$

as the moving point $x_{j-\frac{1}{2}}(t)$ with the speed $w_{j-\frac{1}{2}}$ from t_n to t_{n+1}. Then we define the function $w : \Omega \times [t_n, t_{n+1}] \to \mathbb{R}$ as the grid velocity. It is for any time-dependent cell $K_j(t) = [x_{j-\frac{1}{2}}(t), x_{j+\frac{1}{2}}(t)]$ and $t \in [t_n, t_{n+1}]$ given by

$$w(x,t) = w_{j+\frac{1}{2}}\frac{x - x_{j-\frac{1}{2}}(t)}{h_j(t)} + w_{j-\frac{1}{2}}\frac{x_{j+\frac{1}{2}}(t) - x}{h_j(t)}, \tag{5}$$

where $h_j(t) = x_{j+\frac{1}{2}}(t) - x_{j-\frac{1}{2}}(t)$. In addition, we assume that $w(x,t)$ and $\partial_x w(x,t)$ are bounded in $\Omega \times [0,T]$. Denote the maximal cell length by $h := \max\limits_{t\in[0,T]}\max\limits_{1\leqslant j\leqslant N} h_j(t)$. We assume the mesh is regular, that is, there exists a constant $\sigma > 0$ which is independent of h, such that

$$h_j(t) \geqslant \sigma h, \ \forall j = 1, \cdots, N. \tag{6}$$

Therefore, for any $t \in [t_n, t_{n+1}]$, the cell $K_j(t)$ can be connected with the reference cell $[-1,1]$ by the time-dependent mapping

$$\chi_j : [-1,1] \to K_j(t), \quad \chi_j(\xi,t) = \frac{h_j(t)}{2}(\xi+1) + x_{j-\frac{1}{2}}(t). \tag{7}$$

Thus, we have

$$\partial_t(\chi_j(\xi,t)) = w(\chi_j(\xi,t),t), \quad \forall(\xi,t) \in [-1,1]\times[t_n,t_{n+1}]. \tag{8}$$

Furthermore, the finite element space is defined as

$$V_h := \{v_h \in L^2(\Omega) | v_h(\chi_j(\cdot,t)) \in \mathbb{P}^k([-1,1]), \forall t \in [t_n, t_{n+1}] \ \text{and} \ j = 1,\cdots,N\}, \tag{9}$$

where $\mathbb{P}^k([-1,1])$ denotes the space of polynomials in $[-1,1]$ of degree at most k and the modal basis $\xi^i, i = 0,1,\cdots,k$ could be used in the reference cell. Moreover, we denote the L^2 inner products in $K_j(t)$ and Ω by $(v,w)_j := \int_{K_j(t)} vw\mathrm{d}x$ and $(v,w) := \int_\Omega vw\mathrm{d}x = \sum\limits_j (v,w)_j$, respectively.

Next, we can easily get the transport equation in the approximation space V_h (cf. [24]).

Lemma 1 *Let* $u \in W^{1,\infty}(0,T;H^1(\Omega))$*. Then, for all test functions* $v_h \in V_h$ *where we can choose* v_h *as* $\xi^i \circ \chi_j^{-1}, i = 0, 1, \cdots, k$, *the following transport equation holds*:

$$\frac{\mathrm{d}}{\mathrm{d}t}(u, v_h)_j = (\partial_t u, v_h)_j + (\partial_x(wu), v_h)_j, \tag{10}$$

for all $j = 1, 2, \cdots, N$, *which is owing to*

$$\partial_t v_h(x,t) + w(x,t)\partial_x v_h(x,t) = 0. \tag{11}$$

We first define some notations about norms. Denote $\|v\|_j$ and $\|v\|_{\infty,j}$ as the L^2-norm and L^∞-norm of v on K_j, respectively. Moreover,

$$\|v\|_{l,j} = \left(\sum_{0\leqslant\alpha\leqslant l}\|D^\alpha v\|_j^2\right)^{\frac{1}{2}}, \qquad \|v\|_{l,\infty,j} = \max_{0\leqslant\alpha\leqslant l}\|D^\alpha v\|_{\infty,j},$$

$$\|v\|_l = \left(\sum_j \|v\|_{l,j}^2\right)^{\frac{1}{2}}, \qquad \|v\|_{l,\infty} = \max_j \|v\|_{l,\infty,j},$$

$$\|v\|_\Gamma^2 = \sum_j\left(|v_{j-\frac{1}{2}}^+|^2 + |v_{j-\frac{1}{2}}^-|^2\right).$$

And we express the value of u on the left and right limits of the grid point $x_{j+\frac{1}{2}}(t)$ with $u_{j+\frac{1}{2}}^-$ and $u_{j+\frac{1}{2}}^+$, respectively. Define the jump and the mean of u at $x_{j-\frac{1}{2}}$ as $[u]_{j-\frac{1}{2}} = u_{j-\frac{1}{2}}^+ - u_{j-\frac{1}{2}}^-$ and $\{u\}_{j-\frac{1}{2}} = \frac{u_{j-\frac{1}{2}}^+ + u_{j-\frac{1}{2}}^-}{2}$, respectively.

2.1 The Schemes Related to the L^2 Energy

Rewrite (1) into the following first-order system:

$$\begin{cases} u_t + (f(u))_x + p_x = 0, \\ p - q_x = 0, \\ q - u_x = 0. \end{cases} \tag{12}$$

Then, we adopt the ALE-DG method by Lemma 1 to approximate (12) as follows: find $u_h, p_h, q_h \in V_h(t)$ such that for all test functions $v, r, z \in V_h(t)$,

$$\begin{cases} \frac{\mathrm{d}}{\mathrm{d}t}(u_h, v)_j - (g(\omega, u_h), v_x)_j + \hat{g}_{j+\frac{1}{2}}v_{j+\frac{1}{2}}^- - \hat{g}_{j-\frac{1}{2}}v_{j-\frac{1}{2}}^+ - (p_h, v_x)_j + \hat{p}_{h,j+\frac{1}{2}}v_{j+\frac{1}{2}}^- - \hat{p}_{h,j-\frac{1}{2}}v_{j-\frac{1}{2}}^+ = 0, \\ (p_h, r)_j + (q_h, r_x)_j - \hat{q}_{h,j+\frac{1}{2}}r_{j+\frac{1}{2}}^- + \hat{q}_{h,j-\frac{1}{2}}r_{j-\frac{1}{2}}^+ = 0, \\ (q_h, z)_j + (u_h, z_x)_j - \hat{u}_{h,j+\frac{1}{2}}z_{j+\frac{1}{2}}^- + \hat{u}_{h,j-\frac{1}{2}}z_{j-\frac{1}{2}}^+ = 0, \end{cases} \tag{13}$$

for all j, where $g(\omega,u)=f(u)-\omega u$, $\hat{g}_{j+\frac{1}{2}}=\hat{g}\left(\omega_{j+\frac{1}{2}},u^-_{h,j+\frac{1}{2}},u^+_{h,j+\frac{1}{2}}\right)$ and the "hat" terms are the numerical fluxes. Summing up with respect to j, we obtain

$$\begin{cases}\dfrac{\mathrm{d}}{\mathrm{d}t}(u_h,v)-(g(\omega,u_h),v_x)-\sum\limits_j(\hat{g}[v])_{j-\frac{1}{2}}-(p_h,v_x)-\sum\limits_j(\hat{p}_h[v])_{j-\frac{1}{2}}=0,\\(p_h,r)+(q_h,r_x)+\sum\limits_j(\hat{q}_h[r])_{j-\frac{1}{2}}=0,\\(q_h,z)+(u_h,z_x)+\sum\limits_j(\hat{u}_h[z])_{j-\frac{1}{2}}=0.\end{cases}\tag{14}$$

Next, different kinds of numerical fluxes for linear and nonlinear terms will be discussed. We firstly give several definitions and propositions for the numerical flux of the linear term.

Definition 1 We define the operators $L(\cdot,;\alpha)$, $T(\cdot,\cdot)$ as follows:

$$\begin{cases}L(u,v;\alpha)=-(u,v_x)-\sum\limits_j((\{u\}+\alpha[u])[v])_{j-\frac{1}{2}},\\T(u,v)=(u_t,v)+(\partial_x(wu),v)-\left((\partial_x w)\dfrac{u}{2},v\right),\end{cases}\tag{15}$$

$\forall u,v\in V_h(t)$ and α is a constant.

Definition 2 The operator $N^{\mathrm{d}}(\cdot,\cdot)$ for the nonlinear term $g(\omega,u)$ is defined as

$$N^{\mathrm{d}}(u,v)=-(g(\omega,u),v_x)-\sum_j(\hat{g}[v])_{j-\frac{1}{2}}+\left((\partial_x w)\frac{u}{2},v\right),\forall u,v\in V_h(t),\tag{16}$$

where $\hat{g}=\hat{g}(w,u^-,u^+)$ is a monotone numerical flux. It is a dissipative treatment for the nonlinear term for the L^2 energy.

And we can define the conservative treatment for the nonlinear term as follows.

Definition 3 $\forall u,v\in V_h(t)$, the operator $N^{\mathrm{c}}(:,:)$ is defined as

$$N^{\mathrm{c}}(u,v)=-(g(\omega,u),v_x)-\sum_j(\hat{g}[v])_{j-\frac{1}{2}}+\left((\partial_x w)\frac{u}{2},v\right),\tag{17}$$

where $\hat{g}=\hat{g}(w,v^-,v^+)$ is taken as a conservative flux

$$\hat{g}=\begin{cases}\dfrac{[G(w,u)]}{[u]}, & [u]\neq 0,\\ g(w,u), & [u]=0,\end{cases}\tag{18}$$

where $G(w,u)=\int^u g(w,s)\mathrm{d}s$, especially for $f(u)=u^p$, p is an integer,

$$\hat{g}=\frac{1}{p+1}\sum_{j=0}^{p}(u^-)^j(u^+)^{p-j}-w\{u\}.\tag{19}$$

When $p = 2$, we define the bilinear flux

$$\hat{f}(u, v) = \frac{1}{6}(2u^+v^+ + u^+v^- + u^-v^+ + 2u^-v^-). \tag{20}$$

Therefore, $\hat{g} = \hat{f}(u, u) - w\{u\}$ when $p = 2$. Moreover, we also define a special operator

$$N_{\mathrm{cc}}(u, v; \rho) = -(uv, \rho_x) - \sum_j (\hat{f}(u, v)[\rho])_{j-\frac{1}{2}}. \tag{21}$$

Therefore, $N_{\mathrm{cc}}(u, v; \rho)$ is the Trilinear operator. It is symmetric for variables u and v. It also holds

$$N_{\mathrm{cc}}(u, u; v) + (\omega u, v_x) + \sum_j (\omega\{u\}[v])_{j-\frac{1}{2}} + \left((\partial_x \omega)\frac{u}{2}, v\right) = N^{\mathrm{c}}(u, v). \tag{22}$$

For the dissipative flux, Zhang et al. [40] introduced an important quantity to measure the difference between the numerical flux and the physical flux. In the following lemma, we give the definition.

Lemma 2 *For any monotone numerical flux $\hat{g}$ consistent with g, define*

$$\hat{a}(\hat{g}; v) := \begin{cases} [v]^{-1}(g(\omega, \{v\}) - \hat{g}(\omega, v^-, v^+)), & [v] \neq 0, \\ |g'(\omega, \{v\})|, & [v] = 0. \end{cases}$$

Then, $\hat{a}(\hat{g}; v) \geqslant 0$ and it is bounded for any piecewise smooth function $v \in L^2$. Moreover, we have

$$\begin{cases} \frac{1}{2}|g'(\omega, \{v\})| \leqslant \hat{a}(\hat{g}; v) + C_*|[v]|, \\ -\frac{1}{8}g''(\omega, \{v\})[v] \leqslant \hat{a}(\hat{g}; v) + C_*[v]^2, \end{cases} \tag{23}$$

where the positive constant C_* depends solely on the maximum of $|f''(v)|$ and $|f'''(v)|$.

Remark 1 (Uniformly dissipative flux) For our error estimates, we rewrite the numerical flux in a viscosity form

$$\hat{g}(\omega, v^-, v^+) = \frac{1}{2}(g(\omega, v^-) + g(\omega, v^+) - \lambda(v^-, v^+)(v^+ - v^-)), \tag{24}$$

and assume the viscosity coefficient $\lambda(v^-, v^+)$ satisfies $\lambda(v^-, v^+) \geqslant \lambda_0 > 0$, λ_0 is a constant. The property is necessary due to the lack of control for the jump terms at cell boundaries.

By simple calculations [25], we present several properties of several operators in the following lemma.

Lemma 3 *There hold the equalities*

$$
\begin{cases}
L(u,u;0)=0,\\
L\Big(u,u;-\dfrac{1}{2}\Big)=\sum\limits_{j}\dfrac{1}{2}[u]^2_{j-\frac{1}{2}},\\
L\Big(u,v;\dfrac{1}{2}\Big)=-L\Big(v,u;-\dfrac{1}{2}\Big),\\
L(u,v;0)=-L(v,u;0).
\end{cases}
\tag{25}
$$

In the following lemma, we also present several properties of several operators for the nonlinear term.

Lemma 4 *There hold the equalities*

$$
\begin{cases}
T(u,u)=\dfrac{\mathrm{d}}{\mathrm{d}t}\|u\|^2,\\
N^{\mathrm{d}}(u,u)\geqslant 0,\\
N^{\mathrm{c}}(u,u)=0.
\end{cases}
\tag{26}
$$

Proof We first calculate the first term

$$
\begin{aligned}
\frac{\mathrm{d}}{\mathrm{d}t}\|u\|^2&=\partial_t\left(\frac{u^2}{2},1\right)\\
&=\left(\partial_t\left(\frac{u^2}{2}\right),1\right)+\left(\partial_x\left(\omega\frac{u^2}{2}\right),1\right)\\
&=(u_t,u)+\Big(\partial_x(wu),\frac{u}{2}\Big)+\Big(wu,\partial_x\frac{u}{2}\Big)\\
&=(u_t,u)+\big(\partial_x(wu),u\big)-\Big(\partial_x(wu),\frac{u}{2}\Big)+\Big(wu,\partial_x\frac{u}{2}\Big)\\
&=(u_t,u)+\big(\partial_x(wu),u\big)-\Big((\partial_x w)u,\frac{u}{2}\Big)-\Big(w\partial_x u,\frac{u}{2}\Big)+\Big(wu,\partial_x\frac{u}{2}\Big)\\
&=(u_t,u)+\big(\partial_x(wu),u\big)-\Big((\partial_x w)\frac{u}{2},u\Big)\\
&=T(u,u).
\end{aligned}
\tag{27}
$$

Then we have

$$
\begin{cases}
G(w,u)=\displaystyle\int^u g(w,s)\mathrm{d}s=\int^u f(s)\mathrm{d}s-\frac{w}{2}u^2,\\
\partial_x G(w,u)=f(u)u_x-wuu_x-\partial_x\omega u^2=g(w,u)u_x-\dfrac{\partial_x w}{2}u^2.
\end{cases}
\tag{28}
$$

Therefore,

$$
\begin{cases}
N^{\mathrm{c}}(u,u) = -\big(g(\omega,u),u_x\big) - \sum_j (\hat{g}[u])_{j-\frac{1}{2}} + \left(\left(\partial_x w\right)\frac{u}{2},u\right) \\
\qquad\qquad = -\big(\partial_x G(w,u),1\big) - \sum_j (\hat{g}[u])_{j-\frac{1}{2}} \\
\qquad\qquad = \sum_j \left([G(w,u)] - \frac{[G(w,u)]}{[u]}[u]\right)_{j-\frac{1}{2}} = 0, \\
N^{\mathrm{d}}(u,u) = \sum_j \left(\int_{u^-_{j-\frac{1}{2}}}^{u^+_{j-\frac{1}{2}}} g(w,s)\mathrm{d}s - \hat{g}\int_{u^-_{j-\frac{1}{2}}}^{u^+_{j-\frac{1}{2}}} 1\mathrm{d}s\right) \\
\qquad\qquad = \sum_j \left(\int_{u^-_{j-\frac{1}{2}}}^{u^+_{j-\frac{1}{2}}} (g(w,s) - \hat{g}(w,u^-,u^+))\mathrm{d}s\right) \geqslant 0.
\end{cases}
\tag{29}
$$

The last equation holds because $\hat{g}$ is a monotone flux.

Moreover, for the special operator N_{cc}, we have the following lemma.

Lemma 5 *The operator N_{cc} has the properties as follows.*

(i) *N_{cc} is consistent,*

$$N_{\mathrm{cc}}(u,v;\rho) = ((uv)_x,\rho),\ \textit{for}\ u,v \in C(\Omega),\rho \in V_h(t). \tag{30}$$

(ii) *For $u,v,\rho \in V_h(t)$,*

$$N_{\mathrm{cc}}(u,v;\rho) + N_{\mathrm{cc}}(\rho,u;v) + N_{\mathrm{cc}}(v,\rho;u) = 0. \tag{31}$$

(iii) *For $u,v,\rho \in V_h(t)$,*

$$N_{\mathrm{cc}}(u,v;u) = -\frac{1}{2}N_{\mathrm{cc}}(u,u;v). \tag{32}$$

(iv) *For $u,v,\rho \in V_h(t)$,*

$$N_{\mathrm{cc}}(u,u;u) = 0. \tag{33}$$

Proof

(i) For $u,v \in C(\Omega)$, $\rho \in V_h(t)$, we can easily get (30) by integration by parts and the definition of N_{cc} (21),

$$N_{\mathrm{cc}}(u,v;\rho) = ((uv)_x,\rho) + \sum_j ((uv - \hat{f}(u,v))[\rho])_{j-\frac{1}{2}}.$$

(ii) We can easily verify (31) by integration by parts and the definition of $\hat{f}$ (20).
(iii) The property (32) can be obtained by taking $\rho = u$ in (31) and using the symmetry of the operator N_{cc}.
(iv) Take $v = u$ in (32), we can get the property (33).

Then, we can propose the dissipative and conservative schemes as follows. When choosing $\hat{p}_h = p_h^+, \hat{q}_h = q_h^+, \hat{u}_h = u_h^-$, the dissipative ALE-DG scheme (14) for the first order system (12) can be written as: find $u_h, p_h, q_h \in V_h(t)$ such that for all test functions $v, r, z \in V_h(t)$,

$$\text{NC-NC scheme}\begin{cases} T(u_h, v) + N^{\mathrm{d}}(u_h, v) + L\Big(p_h, v; \dfrac{1}{2}\Big) = 0,\\ (p_h, r) - L\Big(q_h, r; \dfrac{1}{2}\Big) = 0,\\ (q_h, z) - L\Big(u_h, z; -\dfrac{1}{2}\Big) = 0.\end{cases} \tag{34}$$

The scheme satisfies the L^2 stability, which means $\frac{\mathrm{d}}{\mathrm{d}t}\|u_h\|^2 \leqslant 0$. The dissipative scheme destroys the balance between nonlinear steepening and dispersive spreading numerically, it may cause the phase error, shape error and the inaccuracy of the ALE-DG numerical scheme over a long temporal interval.

Next, the conservative scheme will be presented, which preserves the conservation law of the L^2 energy, i.e., $\frac{\mathrm{d}}{\mathrm{d}t}\|u_h\|^2 = 0$. By choosing the numerical fluxes $\hat{p}_h = p_h^+, \hat{q}_h = \{q_h\}, \hat{u}_h = u_h^-$, the L^2 conservative scheme is defined as: find $u_h, p_h, q_h \in V_h(t)$ such that for all test functions $v, r, z \in V_h(t)$,

$$\text{C-C scheme}\begin{cases} T(u_h, v) + N^{\mathrm{c}}(u_h, v) + L\Big(p_h, v; \dfrac{1}{2}\Big) = 0,\\ (p_h, r) - L(q_h, r; 0) = 0,\\ (q_h, z) - L\Big(u_h, z; -\dfrac{1}{2}\Big) = 0.\end{cases} \tag{35}$$

The scheme is conservative for the nonlinear term and linear term, so we denote the scheme by the C-C scheme. The dissipative scheme (34) is denoted by the NC-NC scheme, it is dissipative for the nonlinear term and linear term. We can also denote the C-NC scheme which is conservative for the nonlinear term and dissipative for the linear term: find $u_h, p_h, q_h \in V_h(t)$ such that for all test functions $v, r, z \in V_h(t)$,

$$\text{C-NC scheme}\begin{cases} T(u_h, v) + N^{\mathrm{c}}(u_h, v) + L\Big(p_h, v; \dfrac{1}{2}\Big) = 0,\\ (p_h, r) - L\Big(q_h, r; \dfrac{1}{2}\Big) = 0,\\ (q_h, z) - L\Big(u_h, z; -\dfrac{1}{2}\Big) = 0.\end{cases} \tag{36}$$

We can also denote the NC-C scheme by replacing $L(q_h, r; \frac{1}{2})$ in the scheme (34) with $L(q_h, r; 0)$. The NC-NC, C-NC, NC-C schemes are all the dissipative schemes. Moreover, the flux $\hat{p}_h = p_h^+, \hat{u}_h = u_h^-$ can be defined as $\hat{p}_h = \{p_h\} + \alpha[p_h], \hat{u}_h = \{u_h\} - \alpha[u_h]$ in those schemes. When $\alpha \neq \pm\frac{1}{2}$, it results in a wider stencil. Comparing with the dissipative scheme, the conservative scheme not only has high accuracy and stability, but reduces the phase error and shape error validly over a long temporal interval, especially in low order approximation.

2.2 The Scheme Related to Hamiltonian Energy *H*

In this section, we introduce the Hamiltonian conservative ALE-DG scheme based on the LDG schemes on static grids [29, 41]. Rewrite (1) into the following first-order system:

$$\begin{cases} u_t + (g_p + wu)_x + p_x = 0, \\ p - q_x = 0, \\ q - u_x = 0, \\ g(w,u) - g_p = 0. \end{cases} \tag{37}$$

Then the minimal stencil ALE-DG scheme for (37) is defined: find $u_h, p_h, q_h, g_p \in V_h(t)$ such that for all test functions $v, r, z, s \in V_h(t)$,

$$\text{HC scheme} \begin{cases} \dfrac{\mathrm{d}}{\mathrm{d}t}(u_h, v) + L(g_p, v; 0) + L(p_h, v; 0) = 0, \\ (p_h, r) - L\Big(q_h, r; -\dfrac{1}{2}\Big) = 0, \\ (q_h, z) - L\Big(u_h, z; \dfrac{1}{2}\Big) = 0, \\ (g(w, u_h), s) - (g_p, s) = 0. \end{cases} \tag{38}$$

We can verify that the scheme (38) is a Hamiltonian conservative ALE-DG scheme if the grid velocity function ω is a constant, where $V(u) = G(w, u)$ is in the Hamiltonian energy (2). Then, we have

$$\frac{\mathrm{d}H}{\mathrm{d}t} = (q, q_t) + (q, \omega q_x) - (g(\omega, u), u_t) - (g(\omega, u), \omega u_x). \tag{39}$$

If ω is a constant, we take the time derivative of the third term and rewrite the scheme as

$$\begin{cases} ((u_h)_t + \omega(u_h)_x, v) + L(g_p, v; 0) + L(p_h, v; 0) = 0, \\ (p_h, r) - L\Big(q_h, r; -\dfrac{1}{2}\Big) = 0, \\ ((q_h)_t + \omega(q_h)_x, z) - L\Big((u_h)_t + \omega(u_h)_x, z; \dfrac{1}{2}\Big) = 0, \\ (g(w, u_h), s) - (g_p, s) = 0. \end{cases} \tag{40}$$

Taking the test functions as $v = -(g_p + p_h), r = (u_h)_t + \omega(u_h)_x, z = q_h, s = -((u_h)_t + \omega(u_h)_x)$, we have

$$\begin{cases} ((u_h)_t + \omega(u_h)_x, -(g_p + p_h)) + L(g_p, -(g_p + p_h); 0) + L(p_h, -(g_p + p_h); 0) = 0, \\ (p_h, (u_h)_t + \omega(u_h)_x) - L\Big(q_h, (u_h)_t + \omega(u_h)_x; -\dfrac{1}{2}\Big) = 0, \\ ((q_h)_t + \omega(q_h)_x, q_h) - L\Big((u_h)_t + \omega(u_h)_x, q_h; \dfrac{1}{2}\Big) = 0, \\ (g(u), -((u_h)_t + \omega(u_h)_x)) - (g_p, -((u_h)_t + \omega(u_h)_x)) = 0. \end{cases} \tag{41}$$

Summing up the terms in (41) and using the properties of the operators, we can easily get $\frac{\mathrm{d}H}{\mathrm{d}t}=0$. Unfortunately, when the grid velocity is no longer a constant, we can not get the Hamiltonian conservation of the scheme. Even though, we still call the scheme (38) as HC scheme.

It is worth to mention that another Hamiltonian conservation scheme in [31] can be extended to moving meshes, in which the multi-symplectic form of the Hamiltonian system was adopted to develop the structure preserving DG methods.

3 Error Estimate

In this section, we consider the L^2-norm error estimates for the NC-NC scheme (34) and C-NC scheme (36). For the ALE-DG methods to nonlinear KdV equations, there exist some obstacles in handling the error estimates for linear terms when choosing $\hat{q}_h=\{q_h\}$. We only choose the dissipative flux $\hat{q}_h=q_h^+$ in the following error estimates and consider mainly the NC-NC and C-NC schemes. For NC-NC scheme, we refer to Xu et al. [35] for our error estimates. For the C-NC scheme, we refer to Zhang et al. [39] to estimate our error. Before starting the error estimates, we first give some notations.

3.1 Notations for Projections and Some Properties of Approximation Space

The inverse properties of the finite space V_h will be used.

Lemma 6 *When the mesh is regular,* $\forall v\in V_h,\ \exists C>0,\ s.t.$

$$h^2\|\partial_x v\|^2+h\|v\|_\Gamma^2\leqslant C\|v\|^2, \tag{42}$$

where the positive constant C *is independent of* h *and* v.

Define the L^2-projection P_k, two Gauss-Radau projections P_- and P_+ of u into V_h as follows:

$$\begin{aligned}
&(P_k u, v_h)=(u,v_h), \forall v_h\in V_h \text{ with } v_h(\chi_j(\cdot,t))\in P^k([-1,1]),\\
&(P_- u, v_h)=(u,v_h), \forall v_h\in V_h \text{ with } v_h(\chi_j(\cdot,t))\in P^{k-1}([-1,1]),\ \text{and } (P_-u)^-_{j-\frac{1}{2}}=u^-_{j-\frac{1}{2}},\\
&(P_+ u, v_h)=(u,v_h), \forall v_h\in V_h \text{ with } v_h(\chi_j(\cdot,t))\in P^{k-1}([-1,1]),\ \text{and } (P_+u)^+_{j-\frac{1}{2}}=u^+_{j-\frac{1}{2}}.
\end{aligned}$$

The following lemma states the error of these projections [3].

Lemma 7 *Let* P_h *be a projection, either* P_k, P_- *or* P_+, *and* $P_h^\perp q=q-P_hq$ *be the projection error. For any smooth function* $q(x)$, $\exists c>0$, *such that*

$$\|P_h^\perp q\|_D+h\|\partial_x(P_h^\perp q)\|_D+h^{\frac{1}{2}}\|P_h^\perp q\|_{\infty,D}\leqslant ch^{k+1}|q|_{k+1,D}, \tag{43}$$

$$\|P_h^\perp q\|_\Gamma\leqslant ch^{k+\frac{1}{2}}\|\partial_x^{k+1}q\|, \tag{44}$$

where the positive constant c is not dependent on h, solely depending on q, and D may be Ω or $K_j(t)$.

From [24], we have the following lemmas on the time-dependent projections.

Lemma 8 *Let $\phi \in W^{1,\infty}(0,T;H^1(\Omega))$. Then, it holds that*

$$\partial_t P_h\phi + \Omega\partial_x P_h\phi = P_h(\partial_t\phi) + P_h(\omega\partial_x\phi). \tag{45}$$

Lemma 9 *Let $u \in L^2(\Omega)$ and $v_h \in V_h$, Then, it holds that*

$$(u - P_k u, \partial_t v_h)_j = 0. \tag{46}$$

Furthermore, to avoid the confusion with different constants, we denote a generic positive constant by C, which is independent of the numerical solution and the mesh size for our problem. But, the constant may be dependent on the exact solution and may have a different value in each occurrence. Moreover, for problems considered in this paper, the exact solution is assumed to be smooth with periodic or compactly supported boundary conditions. Therefore, the exact solution is always bounded. We follow the convention [40] to refine the nonlinear function $f(u)$ outside their ranges such that the derivatives $f'(u)$,$f''(u)$ become globally bounded functions.

3.2 L^2-Norm Error Estimate for NC-NC Scheme (34)

We first state the L^2-norm error estimate for the scheme and then give its proof. Similar to the LDG method on static grid [35, 38] , we can get the suboptimal error estimate. However, in the numerical tests we can observe the optimal order of accuracy.

Theorem 1 *Let u be the exact solution of problem* (1), *which is sufficiently smooth with bounded derivatives, and $f \in C^3$. Assume u_h is the ALE-DG approximation of semi-discrete NC-NC scheme* (34) *with the flux* (24) *and the approximation space V_h is the space consisting of k-th piecewise polynomial ($k \geqslant 1$). Assuming $\partial_x w$, w are bounded. Then, it holds that*

$$\|u(T) - u_h(T)\| \leqslant Ch^{k+\frac{1}{2}}, \tag{47}$$

where C is a positive constant independent on h.

Proof To deal with the nonlinearity of the flux $g(u)$ we want to make a priori assumption.

Assumption 1 For a small enough h, it holds

$$\|u - u_h\| \leqslant h. \tag{48}$$

The priori assumption is unnecessary for linear KdV equations.

By Lemmas 6 and 7, Assumption 1 implies

$$\|u_h - P_h u\|_\infty \leqslant ch^{\frac{1}{2}}, \|e_u\|_\infty \leqslant ch^{\frac{1}{2}}, \tag{49}$$

where $e_u = u_h - u$. Notice that the scheme (34) is still satisfied with $u_h = u, p_h = u_{xx}$, $q_h = u_x$. Therefore, we have the error equation

$$N^{\mathrm{d}}(u,v)-N^{\mathrm{d}}(u_h,v)=T(u_h-u,v)+L\Big(p_h-p,v;\frac{1}{2}\Big)+(p_h-p,r)-L\Big(q_h-q,r;\frac{1}{2}\Big) \tag{50}$$

$$+(q_h-q,z)-L\Big(u_h-u,z;-\frac{1}{2}\Big). \tag{51}$$

Define $e_u=u_h-u=(u_h-P\_u)-(u-P\_u)=\tilde{e}_u-P_-^{\perp}u$, $p_h-p=(p_h-P_kp)-(p-P_kp)=\tilde{e}_p-P_k^{\perp}p$, and $q_h-q=(q_h-P_kq)-(q-P_kq)=\tilde{e}_q-P_k^{\perp}q$. Then taking $v=\tilde{e}_u, r=\tilde{e}_q, z=-\tilde{e}_p$, we have

$$\begin{aligned}N^{\mathrm{d}}(u,\tilde{e}_u)-N^{\mathrm{d}}(u_h,\tilde{e}_u)&=T(\tilde{e}_u-P_-^{\perp}u,\tilde{e}_u)+L\Big(\tilde{e}_p-P_k^{\perp}p,\tilde{e}_u;\frac{1}{2}\Big)+(\tilde{e}_p-P_k^{\perp}p,\tilde{e}_q)\\&\quad-L\Big(\tilde{e}_q-P_k^{\perp}q,\tilde{e}_q;\frac{1}{2}\Big)+(\tilde{e}_q-P_k^{\perp}q,-\tilde{e}_p)-L\Big(\tilde{e}_u-P_-^{\perp}u,-\tilde{e}_p;-\frac{1}{2}\Big).\end{aligned} \tag{52}$$

We know the operators T, L are bilinear. By Lemmas 3, 4, the definition of the projections, the right terms RHS of the error (52) become

$$\begin{aligned}\mathrm{RHS}&=T(\tilde{e}_u,\tilde{e}_u)+L\Big(\tilde{e}_p,\tilde{e}_u;\frac{1}{2}\Big)+(\tilde{e}_p,\tilde{e}_q)-L\Big(\tilde{e}_q,\tilde{e}_q,\frac{1}{2}\Big)+(\tilde{e}_q,-\tilde{e}_p)\\&\quad-L\Big(\tilde{e}_u,-\tilde{e}_p;-\frac{1}{2}\Big)-T(P_-^{\perp}u,\tilde{e}_u)-L\Big(P_k^{\perp}p,\tilde{e}_u;\frac{1}{2}\Big)-(P_k^{\perp}p,\tilde{e}_q)\\&\quad+L\Big(P_k^{\perp}q,\tilde{e}_q;\frac{1}{2}\Big)-(P_k^{\perp}q,-\tilde{e}_p)+L\Big(P_-^{\perp}u,-\tilde{e}_p;-\frac{1}{2}\Big)\\&=\frac{1}{2}\frac{\mathrm{d}}{\mathrm{d}t}\|\tilde{e}_u\|^2+\frac{1}{2}\sum_j[\tilde{e}_q]^2_{j-\frac{1}{2}}-T(P_-^{\perp}u,\tilde{e}_u)+\sum_j((P_k^{\perp}p)^+[\tilde{e}_u])_{j-\frac{1}{2}}\\&\quad-\sum_j((P_k^{\perp}q)^+[\tilde{e}_q])_{j-\frac{1}{2}}.\end{aligned} \tag{53}$$

Furthermore, using Lemma 8, we have

$$\begin{aligned}T(P_-^{\perp}u,\tilde{e}_u)&=(\partial_t(P_-^{\perp}u),\tilde{e}_u)+(\partial_x(\omega P_-^{\perp}u),\tilde{e}_u)-\left((\partial_x\omega)\frac{P_-^{\perp}u}{2},\tilde{e}_u\right)\\&=(P_-^{\perp}(\partial_tu+\omega\partial_xu)-\omega\partial_xP_-^{\perp}u,\tilde{e}_u)+((\partial_x\omega)P_-^{\perp}u,\tilde{e}_u)+(\omega\partial_x(P_-^{\perp}u),\tilde{e}_u)-\left((\partial_x\omega)\frac{P_-^{\perp}u}{2},\tilde{e}_u\right)\\&=(P_-^{\perp}(\partial_tu+\omega\partial_xu),\tilde{e}_u)+\frac{1}{2}((\partial_x\omega)P_-^{\perp}u,\tilde{e}_u).\end{aligned} \tag{54}$$

Then, we consider the left term LHS of the error (52),

$$\begin{aligned}\mathrm{LHS}&=N^{\mathrm{d}}(u,\tilde{e}_u)-N^{\mathrm{d}}(u_h,\tilde{e}_u)=-(g(\omega,u),\partial_x\tilde{e}_u)\\&\quad-\sum_j(\hat{g}(w,u)[\tilde{e}_u])_{j-\frac{1}{2}}+\Big((\partial_x\omega)\frac{u}{2},\tilde{e}_u\Big)\\&\quad+(g(\omega,u_h),\partial_x\tilde{e}_u)+\sum_j(\hat{g}(\omega,u_h)[\tilde{e}_u])_{j-\frac{1}{2}}-\Big((\partial_x\omega)\frac{u_h}{2},\tilde{e}_u\Big)\\&=-(g(\omega,u)-g(\omega,u_h),\partial_x\tilde{e}_u)-\sum_j((g(\omega,u)-\hat{g}(w,u_h))[\tilde{e}_u])_{j-\frac{1}{2}}+\frac{1}{2}((\partial_xw)(P_-^{\perp}u-\tilde{e}_u),\tilde{e}_u).\end{aligned} \tag{55}$$

Therefore, the error (52) becomes

$$\frac{1}{2}\frac{\mathrm{d}}{\mathrm{d}t}\|\tilde{e}_u\|^2 + \frac{1}{2}\sum_j [\tilde{e}_q]^2_{j-\frac{1}{2}} = E1 + E2 + E3, \tag{56}$$

where

$$\begin{cases} E1 = (P_-^{\perp}(\partial_t u + \omega\partial_x u), \tilde{e}_u) + \frac{1}{2}((\partial_x\omega)P_-^{\perp}u, \tilde{e}_u) - \frac{1}{2}((\partial_x w)\tilde{e}_u, \tilde{e}_u) - \sum_j ((P_k^{\perp}p)^+[\tilde{e}_u])_{j-\frac{1}{2}} \\ \qquad + \sum_j ((P_k^{\perp}q)^+[\tilde{e}_q])_{j-\frac{1}{2}}, \\ E2 = -\sum_j ((g(\omega, \{u_h\}) - \hat{g}(w, u_h))[\tilde{e}_u])_{j-\frac{1}{2}}, \\ E3 = -(g(\omega, u) - g(\omega, u_h), \partial_x \tilde{e}_u) - \sum_j ((g(\omega, u) - g(w, \{u_h\}))[\tilde{e}_u])_{j-\frac{1}{2}}. \end{cases} \tag{57}$$

Next, the estimates for $E1$, $E2$ and $E3$ are presented in the following, and the proofs are given in Appendixes A, B, and C:

$$E1 \leqslant C(h^{2k+1} + \|\tilde{e}_u\|^2) + \frac{1}{8}\sum_j \hat{a}(\hat{g}; u_h)[\tilde{e}_u]^2_{j-\frac{1}{2}} + \frac{1}{4}\sum_j [\tilde{e}_q]^2_{j-\frac{1}{2}}, \tag{58}$$

$$E2 \leqslant ch^{2k+1} - \frac{3}{4}\sum_j (\hat{a}(\hat{g}; u_h)[\tilde{e}_u]^2)_{j-\frac{1}{2}}, \tag{59}$$

$$E3 \leqslant \frac{1}{2}\sum_j (\hat{a}(\hat{g}; u_h)[\tilde{e}_u]^2)_{j-\frac{1}{2}} + (c + c(\|\tilde{e}_u\|_\infty + h^{-1}\|e_u\|^2_\infty))\|\tilde{e}_u\|^2 + (c + ch^{-1}\|e_u\|^2_\infty)h^{2k+1}. \tag{60}$$

Using (56), (58)–(60), we can obtain

$$\frac{1}{2}\frac{\mathrm{d}}{\mathrm{d}t}\|\tilde{e}_u\|^2 + \frac{1}{4}\sum_j [\tilde{e}_q]^2_{j-\frac{1}{2}} + \frac{1}{8}\sum_j \hat{a}(\hat{g}; u_h)[\tilde{e}_u]^2_{j-\frac{1}{2}} \leqslant c\|\tilde{e}_u\|^2 + ch^{2k+1}, \tag{61}$$

which implies

$$\frac{1}{2}\frac{\mathrm{d}}{\mathrm{d}t}\|\tilde{e}_u\|^2 \leqslant c\|\tilde{e}_u\|^2 + ch^{2k+1}. \tag{62}$$

Thus by Gronwall's inequality, the conclusion in Theorem 1 follows.

To complete the proof we need to justify Assumption 1. Here we use "induction over the continuum" in [21]. There are two steps to verify $||u(t) - u_h(t)|| \leqslant h$ for all $t \leqslant T$.

I. Because $u_h(0)$ is the initial projection, we have $||u(0) - u_h(0)|| \leqslant Ch^{k+1} < h$ for a small enough h. By the continuity of $||u(t) - u_h(t)||$, $\exists\epsilon > 0$, such that $||u(t) - u_h(t)|| \leqslant h, \forall t \in [0, \epsilon)$.

II. For a small enough h, for any $a \leqslant T$, if $||u(t) - u_h(t)|| \leqslant h, \forall t \in [0, a]$, we have proved that $||u(t) - u_h(t)|| \leqslant Ch^{k+\frac{1}{2}}$. Again by the continuity of $||u(t) - u_h(t)||$,

$||u(t)-u_h(t)|| \leqslant Ch^{k+\frac{1}{2}}, \forall t \in [0,a] \Rightarrow \exists b > a, ||u(t)-u_h(t)|| \leqslant h, \forall t \in [0,b)$. This implies $||u(t)-u_h(t)|| \leqslant h, \forall t \in [0,a] \Rightarrow \exists b > a, ||u(t)-u_h(t)|| \leqslant h, \forall t \in [0,b)$.

By those two steps and "induction over the continuum" in [21], we can get $||u(t)-u_h(t)|| \leqslant h, \forall t \in [0,T]$.

3.3 L^2-Norm Error Estimate for C-NC Scheme (36)

We first state the L^2-norm error estimate for C-NC scheme and then give its proof.

Theorem 2 *Let u be the exact solution of problem* (1), *which is sufficiently smooth with bounded derivatives. Assume u_h is the ALE-DG approximation of the semi-discrete C-NC scheme* (36) *and the approximation space V_h is the space consisting of the k-th piecewise polynomial* ($k \geqslant 1$)*. Assuming $\partial_x w$, w is bounded. Then, it holds that*

$$\|u(T)-u_h(T)\| \leqslant Ch^k, \tag{63}$$

where C is a positive constant independent on h.

Proof Equation (56) is still valid,

$$\begin{aligned}
&\frac{1}{2}\frac{\mathrm{d}}{\mathrm{d}t}\|\tilde{e}_u\|^2 + \frac{1}{2}\sum_j [\tilde{e}_q]^2_{j-\frac{1}{2}} \\
&= (P^{\perp}_{-}(\partial_t u + \omega\partial_x u), \tilde{e}_u) + \big((\partial_x\omega)P^{\perp}_{-}u, \tilde{e}_u\big) - \frac{1}{2}\big((\partial_x w)\tilde{e}_u, \tilde{e}_u\big) - \sum_j ((P^{\perp}_k p)^+[\tilde{e}_u])_{j-\frac{1}{2}} \\
&\quad + \sum_j ((P^{\perp}_k q)^+[\tilde{e}_q])_{j-\frac{1}{2}} - (g(\omega,u)-g(\omega,u_h), \partial_x\tilde{e}_u) - \sum_j ((g(\omega,u)-\hat{g}(w,u_h))[\tilde{e}_u])_{j-\frac{1}{2}} \\
&= (P^{\perp}_{-}(\partial_t u + \omega\partial_x u), \tilde{e}_u) + ((\partial_x\omega)P^{\perp}_{-}u, \tilde{e}_u) - \frac{1}{2}((\partial_x w)\tilde{e}_u, \tilde{e}_u) - \sum_j ((P^{\perp}_k p)^+[\tilde{e}_u])_{j-\frac{1}{2}} \\
&\quad + \sum_j ((P^{\perp}_k q)^+[\tilde{e}_q])_{j-\frac{1}{2}} + N_{\mathrm{cc}}(u,u;\tilde{e}_u) - N_{\mathrm{cc}}(u_h,u_h;\tilde{e}_u) + (\omega(u-u_h), (\tilde{e}_u)_x) \\
&\quad + \sum_j (\omega\{u-u_h\}[\tilde{e}_u])_{j-\frac{1}{2}} \\
&= (P^{\perp}_{-}(\partial_t u + \omega\partial_x u), \tilde{e}_u) + ((\partial_x\omega)P^{\perp}_{-}u, \tilde{e}_u) - \frac{1}{2}((\partial_x w)\tilde{e}_u, \tilde{e}_u) - \sum_j ((P^{\perp}_k p)^+[\tilde{e}_u])_{j-\frac{1}{2}} \\
&\quad + \sum_j ((P^{\perp}_k q)^+[\tilde{e}_q])_{j-\frac{1}{2}} + N_{\mathrm{cc}}(u,u;\tilde{e}_u) - N_{\mathrm{cc}}(u_h,u_h;\tilde{e}_u) + (\omega(P^{\perp}_{-}u-\tilde{e}_u), (\tilde{e}_u)_x) \\
&\quad + \sum_j (\omega\{P^{\perp}_{-}u-\tilde{e}_u\}[\tilde{e}_u])_{j-\frac{1}{2}} = (P^{\perp}_{-}(\partial_t u + \omega\partial_x u), \tilde{e}_u) + ((\partial_x\omega)P^{\perp}_{-}u, \tilde{e}_u) + (\omega P^{\perp}_{-}u, (\tilde{e}_u)_x) \\
&\quad + \sum_j ((P^{\perp}_k q)^+[\tilde{e}_q])_{j-\frac{1}{2}} - \sum_j ((P^{\perp}_k p)^+[\tilde{e}_u])_{j-\frac{1}{2}} + \sum_j (\omega\{P^{\perp}_{-}u\}[\tilde{e}_u])_{j-\frac{1}{2}} \\
&\quad - \frac{1}{2}((\partial_x w)\tilde{e}_u, \tilde{e}_u) - (\omega\tilde{e}_u, (\tilde{e}_u)_x) - \sum_j (\omega\{\tilde{e}_u\}[\tilde{e}_u])_{j-\frac{1}{2}} + N_{\mathrm{cc}}(u,u;\tilde{e}_u) - N_{\mathrm{cc}}(u_h,u_h;\tilde{e}_u) \\
&= R1 + R2 + R3 + R4 + R5,
\end{aligned} \tag{64}$$

where

$$
\begin{cases}
R1 = (P_-^{\perp}(\partial_t u + \omega\partial_x u), \tilde{e}_u) + ((\partial_x\omega)P_-^{\perp}u, \tilde{e}_u) + (\omega P_-^{\perp}u, (\tilde{e}_u)_x),\\
R2 = \sum_j ((P_k^{\perp}q)^+[\tilde{e}_q])_{j-\frac{1}{2}},\\
R3 = -\sum_j ((P_k^{\perp}p)^+[\tilde{e}_u])_{j-\frac{1}{2}} + \sum_j (\omega\{P_-^{\perp}u\}[\tilde{e}_u])_{j-\frac{1}{2}},\\
R4 = -\frac{1}{2}((\partial_x w)\tilde{e}_u, \tilde{e}_u) - (\omega\tilde{e}_u, (\tilde{e}_u)_x) - \sum_j (\omega\{\tilde{e}_u\}[\tilde{e}_u])_{j-\frac{1}{2}},\\
R5 = N_{\rm cc}(u, u; \tilde{e}_u) - N_{\rm cc}(u_h, u_h; \tilde{e}_u).
\end{cases}
\tag{65}
$$

By Young's inequality, Lemma 7, $\partial_x w \leqslant c$, Lemma 6 and integrating by parts, we have

$$
\begin{cases}
R1 \leqslant c(h^{2k+2} + \|\tilde{e}_u\|^2),\\
R2 \leqslant c(h^{2k+1}) + \frac{1}{4}\sum_j [\tilde{e}_q]^2_{j-\frac{1}{2}},\\
R3 \leqslant c(h^{2k} + \|\tilde{e}_u\|^2),\\
R4 = 0,\\
R5 = (N_{\rm cc}(u, u; \tilde{e}_u) - N_{\rm cc}(P\_u, P\_u; \tilde{e}_u)) + (N_{\rm cc}(P\_u, P\_u; \tilde{e}_u) - N_{\rm cc}(u_h, u_h; \tilde{e}_u)).
\end{cases}
\tag{66}
$$

Next, we estimate the two terms of $R5$, respectively. By $u_h = \tilde{e}_u + P\_u$, the trilinear property of $N_{\rm cc}$, Lemmas 5 and 6, we have

$$
\begin{aligned}
N_{\rm cc}(P\_u, P\_u; \tilde{e}_u) - N_{\rm cc}(u_h, u_h; \tilde{e}_u) &= N_{\rm cc}(P\_u, P\_u; \tilde{e}_u) - N_{\rm cc}(\tilde{e}_u + P\_u, \tilde{e}_u + P\_u; \tilde{e}_u)\\
&= -N_{\rm cc}(\tilde{e}_u, \tilde{e}_u; \tilde{e}_u) - N_{\rm cc}(\tilde{e}_u, P\_u; \tilde{e}_u) - N_{\rm cc}(P\_u, \tilde{e}_u; \tilde{e}_u)\\
&= N_{\rm cc}(\tilde{e}_u, \tilde{e}_u; P\_u)\\
&= -(\tilde{e}_u^2, \partial_x P\_u) - \sum_j (\hat{f}(\tilde{e}_u, \tilde{e}_u)[P\_u])_{j-\frac{1}{2}}\\
&\leqslant C(\|\partial_x P\_u\|_\infty + h^{-1}\|P_-^{\perp}u\|_\infty)\|\tilde{e}_u\|^2.
\end{aligned}
\tag{67}
$$

Applying Lemma 7 and the smoothness of u, we can get a constant boundary for $\|\partial_x P\_u\|_\infty + h^{-1}\|P_-^{\perp}u\|_\infty$. Therefore, we have

$$
N_{\rm cc}(P\_u, P\_u; \tilde{e}_u) - N_{\rm cc}(u_h, u_h; \tilde{e}_u) \leqslant C\|\tilde{e}_u\|^2. \tag{68}
$$

Then, by using $u = P\_u + P_-^{\perp}u$, the trilinear property, the symmetry of $N_{\rm cc}$, and Lemma 5, we also get

$$
\begin{aligned}
N_{\rm cc}(u, u; \tilde{e}_u) - N_{\rm cc}(P\_u, P\_u; \tilde{e}_u) &= N_{\rm cc}(P\_u + P_-^{\perp}u, P\_u + P_-^{\perp}u; \tilde{e}_u) - N_{\rm cc}(P\_u, P\_u; \tilde{e}_u)\\
&= N_{\rm cc}(P\_u, P_-^{\perp}u; \tilde{e}_u) + N_{\rm cc}(P_-^{\perp}u, P\_u; \tilde{e}_u) + N_{\rm cc}(P_-^{\perp}u, P_-^{\perp}u; \tilde{e}_u)\\
&= 2N_{\rm cc}(P\_u, P_-^{\perp}u; \tilde{e}_u) + N_{\rm cc}(P_-^{\perp}u, P_-^{\perp}u; \tilde{e}_u).
\end{aligned}
\tag{69}
$$

Hence, by Lemma 7, the Cauchy-Schwartz inequality, and Lemma 6, it can easily obtain

$$
\begin{aligned}
N_{\mathrm{cc}}(P\_u, P_-^{\perp}u; \tilde{e}_u) &= -(P\_u(P_-^{\perp}u), \partial_x \tilde{e}_u) - \sum_j (\hat{f}(P\_u, P_-^{\perp}u)[\tilde{e}_u])_{j-\frac{1}{2}} \\
&\leqslant c\|P\_u\|_\infty (\|P_-^{\perp}u\| \|\partial_x \tilde{e}_u\| + \|P_-^{\perp}u\|_\Gamma \|\tilde{e}_u\|_\Gamma) \\
&\leqslant ch^k \|\tilde{e}_u\|
\end{aligned} \tag{70}
$$

and

$$
\begin{aligned}
N_{\mathrm{cc}}(P_-^{\perp}u, P_-^{\perp}u; \tilde{e}_u) &= -(P_-^{\perp}u(P_-^{\perp}u), \partial_x \tilde{e}_u) - \sum_j (\hat{f}(P_-^{\perp}u, P_-^{\perp}u)[\tilde{e}_u])_{j-\frac{1}{2}} \\
&\leqslant c\|P_-^{\perp}u\|_\infty (\|P_-^{\perp}u\| \|\partial_x \tilde{e}_u\| + \|P_-^{\perp}u\|_\Gamma \|\tilde{e}_u\|_\Gamma) \\
&\leqslant ch^{2k+\frac{1}{2}} \|\tilde{e}_u\|.
\end{aligned} \tag{71}
$$

Therefore, we have

$$
N_{\mathrm{cc}}(u, u; \tilde{e}_u) - N_{\mathrm{cc}}(P\_u, P\_u; \tilde{e}_u) \leqslant c(h^{2k} + \|\tilde{e}_u\|^2). \tag{72}
$$

Furthermore,

$$
R5 \leqslant c(h^{2k} + \|\tilde{e}_u\|^2). \tag{73}
$$

Finally, we verify Theorem 2 by Gronwall's inequality.

4 Adaptive Moving Meshes

In this section, we discuss the generation of adaptive moving meshes for problem (1). That is, we want to put more points in the position where the solution changes greatly. We mainly follow Huang et al. [19, 20] and Hong et al. [18]. We firstly denote the reference domain by [0,1] and the physical domain as Ω. The mesh transformation from the reference domain to the physical domain

$$
x : \xi \mapsto x, \ [0,1] \mapsto \Omega
$$

can be obtained by the equidistribution principle

$$
\frac{\mathrm{d}\left(\rho(x)\frac{\mathrm{d}x}{\mathrm{d}\xi}\right)}{\mathrm{d}\xi} = 0, \tag{74}
$$

where $\rho(x)$ is the given positive function which depends on the solution, so called the mesh density function. We discretize (74) with central difference and Gauss-Seidel iteration

$$
\rho\left(u_{j+1}^{[n]}\right)\left(x_{j+\frac{3}{2}}^{[n]} - x_{j+\frac{1}{2}}^{[n+1]}\right) - \rho\left(u_j^{[n]}\right)\left(x_{j+\frac{1}{2}}^{[n+1]} - x_{j-\frac{1}{2}}^{[n+1]}\right) = 0, \tag{75}
$$

where we denote the value of u in the $K_j(t_n)$ by $u_{j+1}^{[n]}$. Clearly, the mesh depends on the mesh density function ρ. The mesh density function is based on the error indicator η_j. Here we adopt an indicator with arbitrary higher order derivative for smooth solutions as in [18],

$$
\begin{cases}
\eta_j^{[n]} = \sum\limits_{l=0}^{k} \left(\left[\partial_x^{(l)} u_h\left(x_{j+\frac{1}{2}}, t\right) \right]^2 + \left[\partial_x^{(l)} u_h\left(x_{j-\frac{1}{2}}, t\right) \right]^2 \right) h_{j+1}^{-(2(k-l)+2)}, \\
\bar{\eta} = \frac{1}{N} \sum\limits_{j=1}^{N} \eta_j^{[n]}, \\
\rho(u_j^{[n]}) = \sqrt{\bar{\eta} + \beta \min\left(\bar{\eta}, \eta_j^{[n]}\right)},
\end{cases} \tag{76}
$$

where β is a mesh quality parameter. We may also choose different indicators according to different situations.

After we get the initial adaptive mesh, to improve the efficiency we adopt the moving mesh partial differential equation (MMPDE) method [19]. In which, the mesh evolves as follows:

$$
\frac{\partial x}{\partial t} = \frac{1}{\tau} \frac{\partial}{\partial \xi} \left(\rho \frac{\partial x}{\partial \xi} \right) = 0, \tag{77}
$$

where the mesh density function is as same as above. For simplicity, we choose the relaxation time parameter $\tau = 1$.

According to this procedure, we can get the mesh which clusteres more grid points to the positions where the solution changes greatly. It is noteworthy that we still need a low-pass filter to improve the mesh smoothness and strict mesh movement restriction to keep the stability. The restriction is to adjust repeatedly the adaptive mesh by reducing the time step to meet the CFL limit.

5 Numerical Experiments

The aims of this section are applying the ALE-DG method on moving meshes to verify the theoretical analysis. For the following numerical examples, the initial discretization is obtained by taking the L^2 projection. And we apply the ALE-DG method with the conservative and dissipative fluxes to the spatial discretization by using P^k polynomials on moving meshes, and divide the domain into N intervals. For the time discretization, we adopt the fourth-order diagonally implicit-explicit additive Runge-Kutta time method in [23, 34], in which the nonlinear term $f(u)_x$ is treated explicitly and the linear dispersive term implicitly. Thus it results in a linear implicit scheme and the time step can be chosen as $\Delta t = \frac{0.1h}{\alpha(2k+1)}$, where $\alpha = \max(f'(u) - w)$ and $h = \min\limits_{1 \leqslant j \leqslant N} h_j(t)$.

Example 1 Soliton wave solution

We compute the classical soliton solution of the KdV equation

$$
\begin{cases}
u_t - 3(u^2)_x + u_{xxx} = 0, \\
u(x, 0) = -2\mathrm{sech}^2(x).
\end{cases} \tag{78}
$$

Clearly, the exact solution is

Table 1 Example 1: ALE-DG schemes according to different fluxes

Scheme	Flux			
	$\hat{g}$	$\hat{p}$	$\hat{q}$	$\hat{u}$
C-C (alternating)	$-(u^+u^+ + u^+u^- + u^-u^-) - w\{u\}$	p^+	$\{q\}$	u^-
C-C (central)	$-(u^+u^+ + u^+u^- + u^-u^-) - w\{u\}$	$\{p\}$	$\{q\}$	$\{u\}$
HC (alternating)	$\{-3u^2 - wu\}$	$\{p\}$	q^-	u^+
HC (central)	$\{-3u^2 - wu\}$	$\{p\}$	$\{q\}$	$\{u\}$
NC-NC	$\frac{g(w,u^+)+g(w,u^-)-\alpha\lvert u^+-u^-\rvert}{2}$	p^+	q^+	u^-
C-NC	$-(u^+u^+ + u^+u^- + u^-u^-) - w\{u\}$	p^+	q^+	u^-

Table 2 Example 1: the L^2 and L^∞-norm errors of the C-C (alternating) type of ALE-DG solutions on the uniform and the moving meshes at $T = 0.5$

	N	Uniform mesh				Moving mesh			
		L^2-error	Order	L^∞-error	Order	L^2-error	Order	L^∞-error	Order
P^1	20	1.31E+00	–	1.11E+00	–	2.63E−01	–	1.70E−01	–
	40	5.80E−01	1.18	3.51E−01	1.66	9.24E−02	1.51	5.89E−02	1.52
	80	2.67E−01	1.12	1.38E−01	1.34	4.15E−02	1.15	1.71E−02	1.78
	160	1.32E−01	1.02	5.49E−02	1.33	2.02E−02	1.04	7.50E−03	1.19
	320	6.56E−02	1.00	2.36E−02	1.22	1.02E−02	0.99	3.80E−03	0.98
P^2	20	4.15E−01	–	3.79E−01	–	1.32E−01	–	9.90E−02	–
	40	7.94E−02	2.39	9.37E−02	2.02	3.35E−03	5.31	6.15E−03	4.01
	80	3.47E−03	4.52	1.01E−02	3.21	3.98E−04	3.07	6.36E−04	3.28
	160	3.75E−04	3.21	1.07E−03	3.25	4.82E−05	3.05	7.71E−05	3.04
	320	4.67E−05	3.01	1.36E−04	2.97	5.71E−06	3.08	9.85E−06	2.97
P^3	20	9.74E−02	–	1.16E−01	–	4.50E−03	–	3.96E−03	–
	40	8.15E−03	3.58	1.37E−02	3.09	5.08E−04	3.15	3.34E−04	3.56
	80	9.44E−04	3.11	1.31E−03	3.38	6.89E−05	2.88	4.02E−05	3.06
	160	1.21E−04	2.97	1.11E−04	3.57	1.03E−05	2.75	5.90E−06	2.77
	320	1.52E−05	2.99	1.11E−05	3.32	1.70E−06	2.59	9.66E−07	2.61

$$u(x,t) = -2\mathrm{sech}^2(x-4t). \tag{79}$$

We simulate this example to time $T = 0.5$ using the periodic boundary conditions on the moving mesh and uniform mesh, respectively. The moving mesh is defined with an initial adaptive mesh with $\beta = 10$ in (76) on $[-15, 17]$ and the grid velocity $w = 4$. The uniform mesh is defined with an initial uniform mesh on $[-15, 17]$ and the grid velocity $w = 0$. Although the exact solution is not periodic, the error produced by the periodic boundary is negligible due to the large size of the computational domain. In addition, to perform the difference of those schemes, we define several types of ALE-DG schemes according to different fluxes in Table 1.

The L^2 and L^∞-norm errors for the P^1, P^2 and P^3 ALE-DG solutions on the moving mesh and the uniform mesh are shown in Tables 2, 3, 4, 5 and 6 for the C-C (alternating), C-C (central), HC (alternating), HC (central) and NC-NC types of schemes, respectively. From the tables, it verifies the $(k+1)$-th order of accuracy for the HC

Table 3 Example 1: the L^2 and L^∞-norm errors of the C-C (central) type of ALE-DG solutions on the uniform and the moving meshes at $T=0.5$

	N	Uniform mesh				Moving mesh			
		L^2-error	Order	L^∞-error	Order	L^2-error	Order	L^∞-error	Order
P^1	20	8.32E−01	–	8.91E−01	–	5.51E−01	–	5.94E−01	–
	40	5.71E−01	0.54	6.06E−01	0.56	2.95E−01	0.90	2.59E−01	1.20
	80	3.43E−01	0.73	4.01E−02	0.60	1.49E−01	0.99	1.35E−01	0.94
	160	1.78E−01	0.95	2.02E−01	0.99	7.55E−02	0.98	6.69E−02	1.01
	320	8.95E−02	0.99	9.78E−02	1.05	3.77E−02	1.00	3.35E−02	1.00
P^2	20	3.30E−01	–	2.40E−01	–	1.10E−01	–	9.18E−02	–
	40	1.35E−01	1.29	2.10E−01	0.19	7.25E−03	3.92	7.00E−03	3.71
	80	5.50E−03	4.62	1.06E−02	4.32	8.70E−04	3.06	9.00E−04	2.96
	160	2.27E−04	4.60	5.90E−04	4.16	1.14E−04	2.93	1.17E−04	2.94
	320	2.72E−05	3.06	6.92E−05	3.09	1.44E−05	2.98	1.48E−05	2.98
P^3	20	1.54E−01	–	1.98E−01	–	1.06E−02	–	7.45E−03	–
	40	1.46E−02	3.40	2.00E−02	3.31	1.06E−03	3.32	8.52E−04	3.13
	80	1.42E−03	3.36	1.71E−03	3.54	1.32E−04	3.00	9.78E−05	3.12
	160	1.85E−04	2.94	2.27E−04	2.91	1.67E−05	2.99	1.32E−05	2.88
	320	2.35E−05	2.98	2.97E−05	2.94	2.10E−06	2.99	1.74E−06	2.93

Table 4 Example 1: the L^2 and L^∞-norm errors of the HC (alernating) type of ALE-DG solutions on the uniform and the moving meshes at $T=0.5$

	N	Uniform mesh				Moving mesh			
		L^2-error	Order	L^∞-error	Order	L^2-error	Order	L^∞-error	Order
P^1	20	2.74E+00	–	1.95E+00	–	8.00E−02	–	1.17E−01	–
	40	1.12E+00	1.29	9.31E−01	1.07	3.25E−02	1.30	5.76E−02	1.02
	80	6.21E−02	4.17	1.06E−01	3.13	7.58E−03	2.10	1.77E−02	1.70
	160	1.33E−02	2.22	2.51E−02	2.08	1.55E−03	2.29	3.51E−03	2.34
	320	3.16E−03	2.07	6.32E−03	1.99	4.08E−04	1.93	9.44E−04	1.89
P^2	20	4.28E+00	–	2.96E+00	–	1.62E−02	–	3.06E−02	–
	40	5.80E−02	6.21	4.05E−02	6.19	1.93E−03	3.07	3.35E−03	3.19
	80	2.42E−03	4.58	5.06E−03	3.00	1.98E−04	3.29	3.46E−04	3.27
	160	2.80E−04	3.11	6.37E−04	2.99	2.47E−05	3.00	4.34E−05	2.99
	320	3.50E−05	3.00	8.07E−05	2.98	3.08E−06	3.00	5.50E−06	2.98
P^3	20	1.15E−01	–	6.45E−02	–	1.75E−03	–	1.69E−03	–
	40	3.60E−03	5.00	3.49E−03	4.21	1.33E−04	3.71	1.26E−04	3.75
	80	1.70E−04	4.41	3.55E−04	3.30	8.96E−06	3.90	8.47E−06	3.89
	160	1.00E−05	4.08	2.16E−05	4.04	4.68E−07	4.26	5.18E−07	4.03
	320	6.29E−07	4.00	1.43E−06	3.91	3.16E−08	3.89	3.77E−08	3.78

Table 5 Example 1: the L^2 and L^∞-norm errors of the HC (central) type of ALE-DG solutions on the uniform and the moving meshes at $T = 0.5$

	N	Uniform mesh				Moving mesh			
		L^2-error	Order	L^∞-error	Order	L^2-error	Order	L^∞-error	Order
P^1	20	5.09E−01	–	6.56E−01	–	2.32E−01	–	2.46E−01	–
	40	1.78E−01	1.52	1.85E−01	1.83	9.24E−02	1.33	1.33E−01	0.89
	80	9.97E−02	0.83	1.14E−01	0.71	4.18E−02	1.14	4.68E−02	1.50
	160	4.56E−02	1.13	5.12E−02	1.15	2.28E−02	0.88	2.72E−02	0.78
	320	2.01E−02	1.18	1.98E−02	1.37	1.12E−02	1.02	1.25E−02	1.12
P^2	20	1.13E+00	–	1.35E+00	–	1.23E−01	–	1.50E−01	–
	40	8.81E−02	3.69	7.37E−02	4.20	1.52E−03	6.34	2.95E−03	5.67
	80	3.02E−03	4.87	6.12E−03	3.59	1.96E−04	2.96	3.91E−04	2.91
	160	2.26E−04	3.74	5.89E−04	3.38	2.50E−05	2.97	4.99E−05	2.97
	320	2.72E−05	3.06	6.92E−05	3.09	3.19E−06	2.97	6.30E−06	2.98
P^3	20	1.15E−01	–	8.21E−02	–	1.78E−03	–	2.35E−03	–
	40	2.90E−03	5.30	5.04E−03	4.03	2.11E−04	3.07	2.68E−04	3.13
	80	2.51E−04	3.53	5.14E−04	3.29	2.45E−05	3.11	3.29E−05	3.03
	160	3.21E−05	2.97	7.85E−05	2.71	3.52E−06	2.80	4.68E−06	2.81
	320	4.37E−06	2.87	8.87E−06	3.15	4.91E−07	2.84	5.34E−07	3.13

Table 6 Example 1: the L^2 and L^∞-norm errors of the NC-NC type of ALE-DG solutions on the uniform and the moving meshes at $T = 0.5$

	N	Uniform mesh				Moving mesh			
		L^2-error	Order	L^∞-error	Order	L^2-error	Order	L^∞-error	Order
P^1	20	9.35E−01	–	7.80E−01	–	1.96E−01	–	2.13E−01	–
	40	3.30E−01	1.50	2.91E−01	1.42	3.77E−02	2.38	4.40E−02	2.28
	80	6.96E−02	2.25	8.21E−02	1.83	7.55E−03	2.32	1.41E−02	1.64
	160	1.22E−02	2.52	1.89E−02	2.12	1.75E−03	2.11	3.97E−03	1.83
	320	2.50E−03	2.28	5.78E−03	1.71	4.29E−04	2.03	1.04E−03	1.93
P^2	20	2.27E−01	–	1.91E−01	–	1.53E−02	–	2.71E−02	–
	40	2.85E−02	2.99	3.51E−02	2.44	2.01E−03	2.93	4.45E−03	2.61
	80	2.95E−03	3.27	8.27E−03	2.09	2.59E−04	2.95	5.88E−04	2.92
	160	3.70E−04	3.00	1.05E−03	2.98	3.27E−05	2.99	7.37E−05	2.99
	320	4.65E−05	2.99	1.40E−04	2.95	4.10E−06	3.00	9.23E−06	3.00
P^3	20	6.01E−02	–	6.60E−02	–	1.89E−03	–	4.59E−03	–
	40	3.60E−03	4.06	1.15E−02	2.51	1.38E−04	3.78	2.84E−04	4.02
	80	2.26E−04	4.00	9.21E−04	3.65	9.26E−06	3.89	2.00E−05	3.83
	160	1.45E−05	3.96	5.65E−05	4.03	5.91E−07	3.97	1.45E−06	3.78
	320	9.12E−07	3.99	3.74E−06	3.92	3.71E−08	3.99	1.00E−07	3.86

Table 7 Example 1: the L^2 and L^∞-norm errors of the NC-NC type of ALE-DG solutions on the uniform and adaptive meshes at $T = 0.5$

	N	Uniform mesh				Adaptive mesh			
		L^2-error	Order	L^∞-error	Order	L^2-error	Order	L^∞-error	Order
P^1	20	9.35E−01	–	7.80E−01	–	2.07E−01	–	2.24E−01	–
	40	3.30E−01	1.50	2.91E−01	1.42	3.73E−02	2.47	4.14E−02	2.44
	80	6.96E−02	2.25	8.21E−02	1.83	7.54E−03	2.31	1.24E−02	1.74
	160	1.22E−02	2.52	1.89E−02	2.12	1.73E−03	2.12	3.39E−03	1.87
	320	2.50E−03	2.28	5.78E−03	1.71	4.20E−04	2.04	8.90E−04	1.92
P^2	20	2.27E−01	–	1.91E−01	–	1.64E−02	–	3.06E−02	–
	40	2.85E−02	2.99	3.51E−02	2.44	2.48E−03	2.72	4.83E−03	2.66
	80	2.95E−03	3.27	8.27E−03	2.09	3.10E−04	2.98	5.13E−04	3.24
	160	3.70E−04	3.00	1.05E−03	2.98	3.92E−05	3.00	6.72E−05	2.93
	320	4.65E−05	2.99	1.40E−04	2.95	4.95E−06	2.99	8.36E−06	3.01
P^3	20	6.01E−02	–	6.60E−02	–	1.98E−03	–	4.57E−03	–
	40	3.60E−03	4.06	1.15E−02	2.51	2.39E−04	3.05	4.55E−04	3.33
	80	2.26E−04	4.00	9.21E−04	3.65	2.05E−05	3.55	5.12E−05	3.15
	160	1.45E−05	3.96	5.65E−05	4.03	1.26E−06	4.02	3.04E−06	4.08
	320	9.12E−07	3.99	3.74E−06	3.92	7.89E−08	4.00	1.75E−07	4.11

Table 8 Example 1: the L^2 and L^∞-norm errors of the C-NC type of ALE-DG solutions on the uniform and adaptive meshes at $T = 0.5$

	N	Uniform mesh				Adaptive mesh			
		L^2-error	Order	L^∞-error	Order	L^2-error	Order	L^∞-error	Order
P^1	20	8.10E−01	–	8.57E−01	–	1.38E−01	–	1.64E−01	–
	40	2.02E−01	2.00	2.61E−01	1.71	2.92E−02	2.24	5.09E−02	1.68
	80	4.34E−02	2.22	8.04E−02	1.70	6.87E−03	2.09	1.40E−02	1.87
	160	9.72E−03	2.16	2.35E−02	1.77	1.68E−03	2.03	3.57E−03	1.97
	320	2.35E−03	2.05	6.32E−03	1.90	4.16E−04	2.01	9.15E−04	1.96
P^2	20	1.84E−01	–	1.47E−01	–	1.64E−02	–	3.49E−02	–
	40	3.13E−02	2.56	4.52E−02	1.70	2.48E−03	2.73	4.83E−03	2.85
	80	2.95E−03	3.41	8.42E−03	2.43	3.14E−04	2.99	5.13E−04	3.24
	160	3.71E−04	2.99	1.06E−03	2.99	3.93E−05	3.00	6.72E−05	2.93
	320	4.65E−05	3.00	1.36E−04	2.97	4.95E−06	2.99	8.36E−06	3.01
P^3	20	6.26E−02	–	6.17E−02	–	2.01E−03	–	4.65E−03	–
	40	3.88E−03	4.01	1.20E−02	2.36	2.40E−04	3.07	4.56E−04	3.35
	80	2.28E−04	4.09	9.28E−04	3.70	2.05E−05	3.55	5.12E−05	3.15
	160	1.45E−05	3.97	5.66E−05	4.03	1.27E−06	4.02	3.04E−06	4.08
	320	9.12E−07	3.99	3.74E−06	3.92	7.89E−08	4.00	1.75E−07	4.11

(alternating) and NC-NC types of ALE-DG solutions both on the uniform and the moving meshes. We can only get the k-th order of accuracy for the C-C (alternating), C-C (central), and HC (central) types of ALE-DG solutions both on the uniform and the moving meshes when k is odd. For the same mesh size N of all those schemes, the error of the ALE-DG solution on the moving mesh is much smaller than that on the uniform mesh because more grid points were put into the area where the solution changes quickly. Moreover, the L^2 and L^∞-norm errors for the P^1, P^2 and P^3 ALE-DG solutions on the adaptive mesh and the uniform mesh are shown in Tables 7 and 8 for the NC-NC and C-NC types of schemes, respectively, where the adaptive meshes are obtained by Sect. 4. It is also shown that the error of the ALE-DG solution on the moving mesh is much smaller than that on the uniform mesh due to the mesh adaption.

Example 2 Nonlinear: cnoidal wave case

We consider the nonlinear KdV equation by setting $\varepsilon = 1/24^2$,

Table 9 Example 2: the L^2 and L^∞-norm errors of the NC-NC, HC (alternating), C-C (alternating) type of P^2 ALE-DG solutions on the uniform and the moving meshes at $T = 1$

	N	Uniform mesh				Moving mesh			
		L^2-error	Order	L^∞-error	Order	L^2-error	Order	L^∞-error	Order
NC-NC	20	6.33E−03	–	1.58E−02	–	1.99E−03	–	5.06E−03	–
	40	3.85E−04	4.04	1.91E−03	3.05	1.92E−04	3.37	8.08E−04	2.65
	80	4.31E−05	3.16	2.72E−04	2.81	2.38E−05	3.01	1.12E−04	2.85
	160	5.38E−06	3.00	3.51E−05	2.95	2.99E−06	2.99	1.48E−05	2.92
	320	6.73E−07	3.00	4.43E−06	2.99	3.75E−07	3.00	1.90E−06	2.96
HC (alternating)	20	2.32E−03	–	1.06E−02	–	1.25E−03	–	3.99E−03	–
	40	2.59E−04	3.16	1.32E−03	3.01	1.48E−04	3.07	5.45E−04	2.87
	80	3.24E−05	3.00	1.69E−04	2.96	1.79E−05	3.05	6.70E−05	3.02
	160	4.05E−06	3.00	2.11E−05	3.00	2.25E−06	3.00	8.81E−06	2.93
	320	5.05E−07	3.00	2.68E−06	2.98	2.82E−07	3.00	1.18E−06	2.90
HC (central)	20	5.45E−03	–	2.36E−02	–	1.48E−03	–	5.76E−03	–
	40	2.21E−04	4.62	1.31E−03	4.17	1.24E−04	3.57	5.21E−04	3.47
	80	2.54E−05	3.12	1.46E−04	3.16	1.54E−05	3.01	7.05E−05	2.89
	160	3.13E−06	3.02	1.79E−05	3.03	1.96E−06	2.98	1.05E−05	2.74
	320	3.89E−07	3.01	2.22E−06	3.01	2.34E−07	3.06	1.36E−06	2.96
C-C (alternating)	20	5.99E−03	–	2.18E−02	–	1.91E−02	–	7.02E−02	–
	40	3.50E−04	4.10	2.32E−03	3.23	7.78E−03	1.29	2.58E−02	1.44
	80	4.33E−05	3.02	2.85E−04	3.02	9.25E−04	3.01	3.14E−03	3.04
	160	5.40E−06	3.00	3.55E−05	3.01	1.12E−04	3.04	3.85E−04	3.03
	320	3.89E−07	3.79	2.22E−06	4.00	1.39E−05	3.02	4.76E−05	3.01
C-C (central)	20	8.03E−03	–	3.41E−02	–	2.68E−02	–	6.78E−02	–
	40	2.24E−04	5.16	1.32E−03	4.70	7.33E−03	1.87	1.74E−02	1.96
	80	2.54E−05	3.14	1.46E−04	3.17	9.21E−04	2.99	2.21E−03	2.98
	160	3.13E−06	3.02	1.79E−05	3.04	1.15E−04	3.00	2.76E−04	3.00
	320	3.89E−07	3.01	2.22E−06	3.01	1.44E−05	3.00	3.43E−05	3.01

Table 10 Example 2: the L^2 and L^∞-norm errors of the NC-NC, HC (alternating), C-C (alternating) type of P^2 ALE-DG solutions on the uniform and the moving meshes at $T = 10$

	N	Uniform mesh				Moving mesh			
		L^2-error	Order	L^∞-error	Order	L^2-error	Order	L^∞-error	Order
NC-NC	20	4.23E−01	–	7.16E−01	–	1.16E−01	–	1.99E−01	–
	40	1.66E−02	4.68	2.85E−02	4.65	4.05E−03	4.84	7.19E−03	4.79
	80	5.35E−04	4.95	1.00E−03	4.83	1.31E−04	4.95	2.56E−04	4.81
	160	1.76E−05	4.92	4.09E−05	4.62	5.18E−06	4.66	1.65E−05	3.96
	320	1.35E−06	3.71	3.60E−06	3.50	3.81E−07	3.76	1.92E−06	3.10
HC (alternating)	20	8.02E−03	–	2.28E−02	–	2.25E−02	–	4.08E−02	–
	40	2.61E−04	4.94	1.42E−03	4.01	9.01E−04	4.64	1.77E−03	4.53
	80	3.23E−05	3.01	1.68E−04	3.07	3.28E−05	4.78	8.46E−05	4.38
	160	4.04E−06	3.00	2.12E−05	2.98	2.36E−06	3.80	9.07E−06	3.22
	320	5.22E−07	2.95	2.91E−06	2.87	3.75E−07	2.65	1.58E−06	2.52
HC (central)	20	3.07E−02	–	6.43E−02	–	4.69E−03	–	1.19E−02	–
	40	4.13E−04	6.21	1.75E−03	5.20	1.39E−04	5.08	5.67E−04	4.40
	80	2.62E−05	3.98	1.52E−04	3.52	1.49E−05	3.22	6.71E−05	3.08
	160	3.12E−06	3.07	1.77E−05	3.10	2.03E−06	2.87	8.80E−06	2.93
	320	4.16E−07	2.91	1.98E−06	3.16	3.62E−07	2.49	1.22E−06	2.85
C-C (alternating)	20	2.01E−01	–	5.04E−01	–	3.15E−01	–	7.84E−01	–
	40	3.81E−04	9.04	2.53E−03	7.64	1.40E−01	1.17	2.95E−01	1.41
	80	4.34E−05	3.13	2.87E−04	3.14	1.60E−02	3.13	5.26E−02	2.49
	160	5.39E−06	3.01	3.54E−05	3.02	1.47E−03	3.45	4.89E−03	3.43
	320	8.12E−07	2.73	5.09E−06	2.80	1.58E−04	3.22	5.25E−04	3.22
C-C (central)	20	5.50E−02	–	1.06E−01	–	4.59E−01	–	1.07E+00	–
	40	5.01E−04	6.78	1.89E−03	5.81	8.15E−02	2.49	2.31E−01	2.21
	80	2.66E−05	4.23	1.54E−04	3.61	9.22E−03	3.14	2.22E−02	3.37
	160	3.12E−06	3.09	1.78E−05	3.12	1.15E−03	3.00	2.69E−03	3.05
	320	4.15E−07	2.91	1.98E−06	3.16	1.44E−04	3.00	3.36E−04	3.00

$$u_t + \frac{1}{2}(u^2)_x + \varepsilon u_{xxx} = 0. \tag{80}$$

The computational domain is [0, 1], and we use the cnoidal-wave solution to check the accuracy. The analytic solution is

$$u(x,t) = a\,\mathrm{cn}^2(4K(x - vt - x_0)), \tag{81}$$

where

$$\begin{cases} a = 192m\varepsilon K^2(m), \\ v = 64\varepsilon(2m-1)K^2(m). \end{cases} \tag{82}$$

The function $\mathrm{cn}(z) = \mathrm{cn}(z; m)$ is the Jacobi elliptic function with modulus $m \in (0, 1)$ (see, [1]). In the numerical experiment, we take $m = 0.9$ and $K = K(m)$ is the complete elliptic integral of the first kind. We take the parameter x_0 as zero and 1 is the spatial period

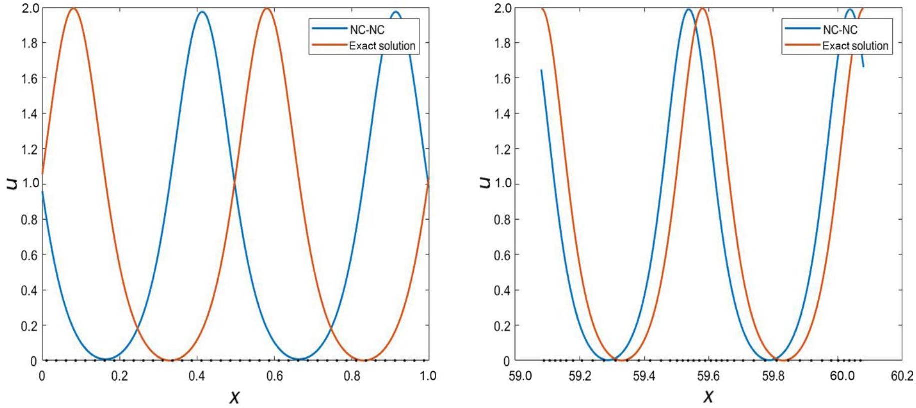

Fig. 1 Example 2: the NC-NC type of ALE-DG solutions u with $N = 40$, P^2 polynomial at $T = 100$ on the static uniform mesh (left) and the moving mesh (right), respectively

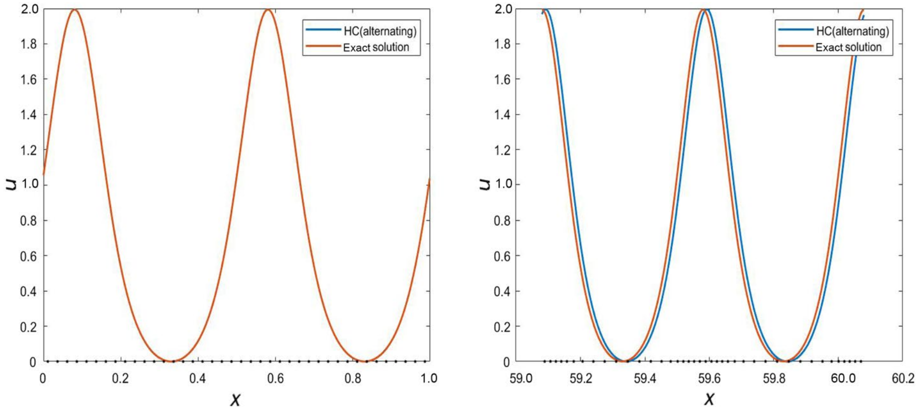

Fig. 2 Example 2: the HC (alternating) type of ALE-DG solutions u with $N = 40$, P^2 polynomial at $T = 100$ on the static uniform mesh (left) and the moving mesh (right), respectively

of the solution. The moving mesh is defined with an initial adaptive mesh with $\beta = 4$ in (76) on [0, 1] and the grid velocity $w = v$. The L^2 and L^∞-norm errors of the NC-NC, HC(alternating), HC(central), C-C(alternating), and C-C(central) type of P^2 ALE-DG solutions on the static uniform and the moving meshes are shown in Table 9 at $T = 1$ and Table 10 at $T = 10$, respectively. We can get the optimal order convergence for the ALE-DG solution on both meshes. Besides, for NC-NC and HC type of schemes, the errors on the moving mesh are smaller than that on the static uniform mesh. For the long time simulation, the adaptive moving mesh can help the dissipative NC-NC scheme to reduce the phase error in Fig. 1. For the HC schemes, especially HC (central) scheme, the adaptive moving mesh works quite well, which does not suffer the artificial oscillations, as shown in Figs. 2 and 3. For the C-C (alternating) scheme, the situation is exactly the opposite. It may be due to the lack of damping mechanism in the L^2 energy conservative C-C schemes, which leads to the artificial oscillations increasing with time evolution, see also Figs. 4, 5

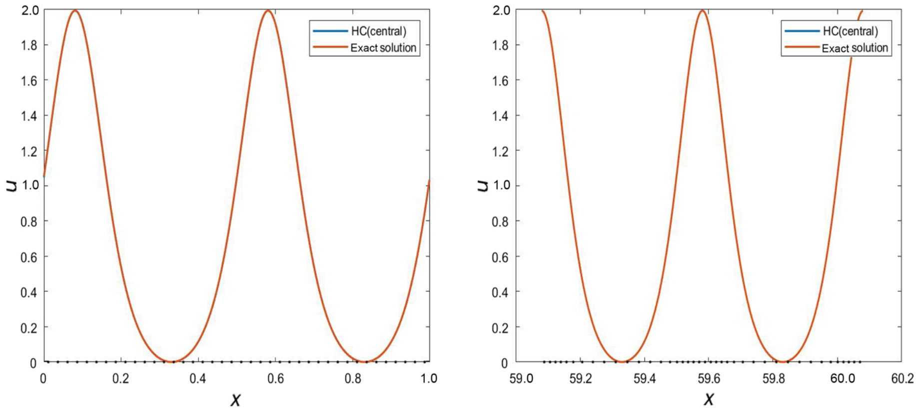

Fig. 3 Example 2: the HC (central) type of ALE-DG solutions u with $N = 40$, P^2 polynomial at $T = 100$ on the static uniform mesh (left) and the moving mesh (right), respectively

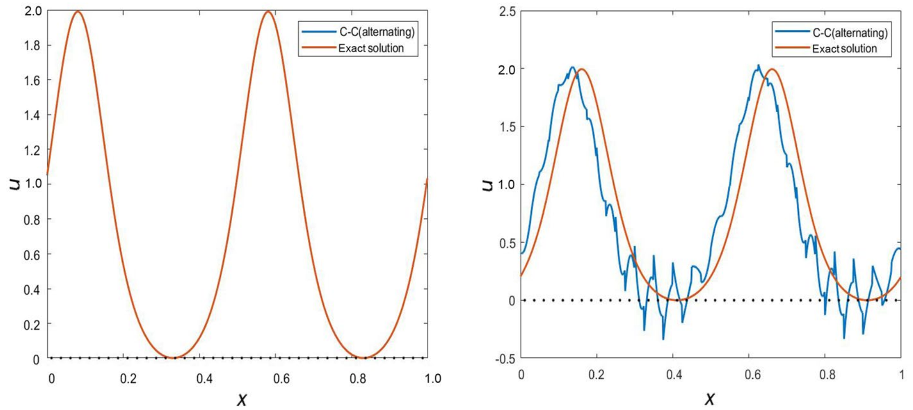

Fig. 4 Example 2: the C-C (alternating) type of ALE-DG solutions u with $N = 40$, P^2 polynomial on the static uniform mesh at $T = 100$ (left) and $T = 200$ (right), respectively

and 6 for long time simulations. And these artificial oscillations could be amplified by the mesh movement, see Figs. 5 and 7.

6 Concluding Remarks

In this paper, we developed and analyzed the conservative and dissipative ALE-DG methods to solve KdV type equations. We also investigated the L^2-norm error estimates for two dissipative schemes. Numerically, we demonstrated the stability and the accuracy of different ALE-DG solutions in accordance with the theoretical analysis. These results also show that the ALE-DG method has better performance on adaptive moving meshes than static meshes.

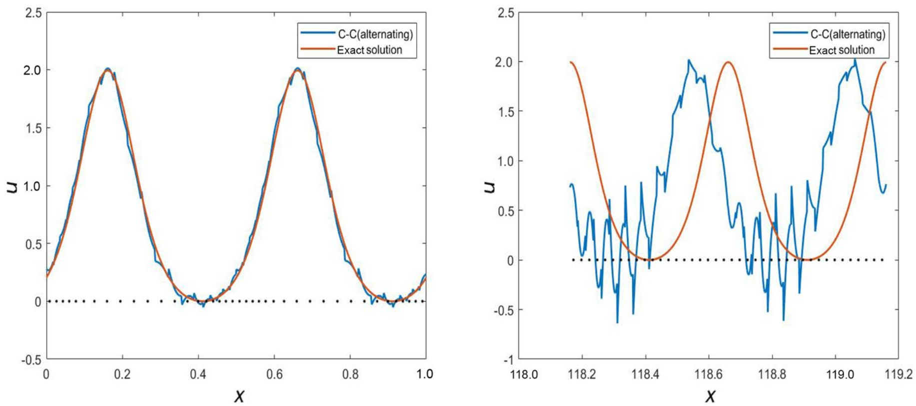

Fig. 5 Example 2: the C-C (alternating) type of ALE-DG solutions u with $N = 40$, P^2 polynomial at $T = 200$ on the mesh with static non-uniform mesh, $w = 0$ (left) and the moving uniform mesh, $w = v$ (right), respectively

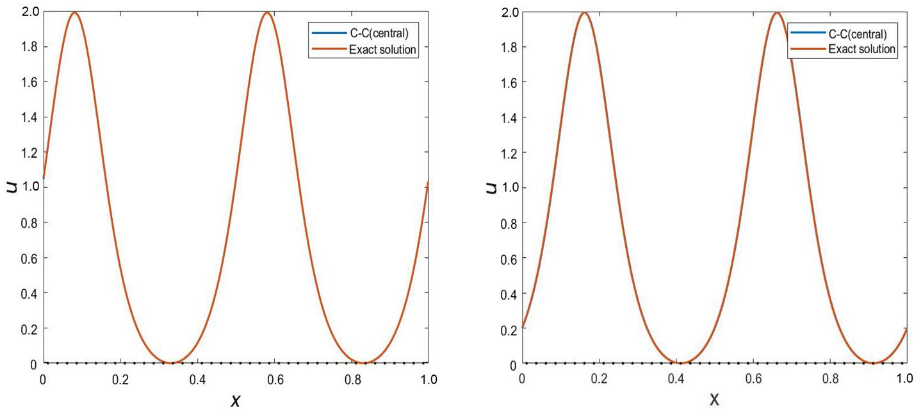

Fig. 6 Example 2: the C-C (central) type of ALE-DG solutions u with $N = 40$, P^2 polynomial on the static uniform mesh at $T = 100$ (left) and $T = 200$ (right), respectively

Appendix A Proof of the Estimate (58)

First, we give the estimate of $E1$ by Young's inequality and Lemma 7.

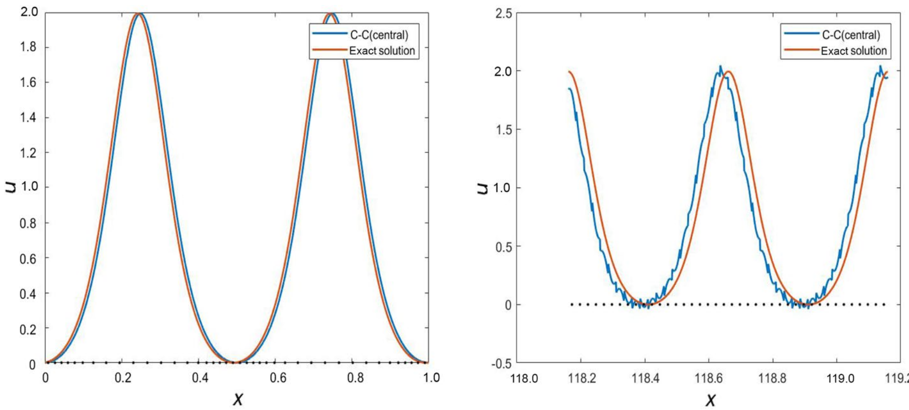

Fig. 7 Example 2: the C-C (central) type of ALE-DG solutions u with $N = 40$, P^2 polynomial at $T = 300$ on the mesh with initial adaptive mesh, $w = 0$ (left) and $T = 200$ with initial uniform mesh, $w = v$ (right), respectively

$$
\begin{aligned}
E1 \leqslant\ & \|P_-^{\perp}(\partial_t u + \omega\partial_x u)\|\|\tilde{e}_u\| + \frac{1}{2}\|\partial_x\omega\|_\infty\|P_-^{\perp}u\|\|\tilde{e}_u\| + \frac{1}{2}\|\partial_x w\|_\infty\|\tilde{e}_u\|^2 \\
& + C\|P_k^{\perp}p\|_\Gamma\left(\sum_j(\hat{a}^{\frac{1}{2}}(\hat{g};u_h)[\tilde{e}_u]_{j-\frac{1}{2}})^2\right)^{\frac{1}{2}} + \|P_k^{\perp}q\|_\Gamma\left(\sum_j[\tilde{e}_q]^2_{j-\frac{1}{2}}\right)^{\frac{1}{2}} \\
\leqslant\ & C(\|P_-^{\perp}(\partial_t u + \omega\partial_x u)\|^2 + \|\tilde{e}_u\|^2 + \|P_-^{\perp}u\|^2 + \|P_k^{\perp}p\|_\Gamma^2 + \|P_k^{\perp}q\|_\Gamma^2) \\
& + \frac{1}{8}\sum_j \hat{a}(\hat{g};u_h)[\tilde{e}_u]^2_{j-\frac{1}{2}} + \frac{1}{4}\sum_j[\tilde{e}_q]^2_{j-\frac{1}{2}} \\
\leqslant\ & C(h^{2k+1} + \|\tilde{e}_u\|^2) + \frac{1}{8}\sum_j \hat{a}(\hat{g};u_h)[\tilde{e}_u]^2_{j-\frac{1}{2}} + \frac{1}{4}\sum_j[\tilde{e}_q]^2_{j-\frac{1}{2}}.
\end{aligned} \tag{A1}
$$

Appendix B Proof of the Estimate (59)

By Lemma 2 and Young's inequality, we have

$$
\begin{aligned}
E2 &= -\sum_j \hat{a}(\hat{g};u_h)[u_h][\tilde{e}_u] = -\sum_j \hat{a}(\hat{g};u_h)[u_h - u][\tilde{e}_u] \\
&= \sum_j \hat{a}(\hat{g};u_h)[P_-^{\perp}u - \tilde{e}_u][\tilde{e}_u] \\
&\leqslant \sum_j(\hat{a}(\hat{g};u_h)[P_-^{\perp}u]^2)_{j-\frac{1}{2}} + \frac{1}{4}\sum_j(\hat{a}(\hat{g};u_h)[\tilde{e}_u]^2)_{j-\frac{1}{2}} - \sum_j(\hat{a}(\hat{g};u_h)[\tilde{e}_u]^2)_{j-\frac{1}{2}} \\
&\leqslant ch^{2k+1} - \frac{3}{4}\sum_j(\hat{a}(\hat{g};u_h)[\tilde{e}_u]^2)_{j-\frac{1}{2}}.
\end{aligned} \tag{B1}
$$

Appendix C Proof of the Estimate (60)

We mainly refer the work [35] to estimate (60). We first use the Taylor expansions and $e_u = u_h - u = \tilde{e}_u - P_-^{\perp}u$,

$$\begin{cases} g(\omega, u_h) - g(\omega, u) = g'(u)(\tilde{e}_u - P_-^{\perp}u) + \dfrac{g''(u)}{2}(\tilde{e}_u - P_-^{\perp}u)^2 + \dfrac{g_u'''}{6}(\tilde{e}_u - P_-^{\perp}u)^3, \\ g(\omega, \{u_h\}) - g(\omega, u) = g'(u)(\{\tilde{e}_u - P_-^{\perp}u\}) + \dfrac{g''(u)}{2}(\{\tilde{e}_u - P_-^{\perp}u\})^2 + \dfrac{\tilde{g}_u'''}{6}(\{\tilde{e}_u - P_-^{\perp}u\})^3, \end{cases} \tag{C1}$$

where $g'(u), g''(u)$ are the derivatives of $g(w, u)$ to the variable u and $g_u''', \tilde{g}_u'''$ are the mean values. In fact, $g'(u) = f'(u) - w, g''(u) = f''(u)$. Then, we have the following representation:

$$\begin{aligned} E3 &= (g(\omega, u_h) - g(w, u), \partial_x \tilde{e}_u) + \sum_j ((g(\omega, \{u_h\}) - g(\omega, u))[u_h])_{j-\frac{1}{2}} \\ &= \mu_1 + \mu_2 + \mu_3 + \mu_4 + \mu_5 + \mu_6, \end{aligned} \tag{C2}$$

where

$$\begin{cases} \mu_1 = (g'(u)\tilde{e}_u, \partial_x \tilde{e}_u) + \sum_j (g'(u)\{\tilde{e}_u\}[\tilde{e}_u])_{j-\frac{1}{2}}, \\ \mu_2 = -(g'(u)P_-^{\perp}u, \partial_x \tilde{e}_u) - \sum_j (g'(u)\{P_-^{\perp}u\}[\tilde{e}_u])_{j-\frac{1}{2}}, \\ \mu_3 = \dfrac{1}{2}(g''(u)\tilde{e}_u^2, \partial_x \tilde{e}_u) + \dfrac{1}{2}\sum_j (g''(u)\{\tilde{e}_u\}^2[\tilde{e}_u])_{j-\frac{1}{2}}, \\ \mu_4 = -(g''(u)\tilde{e}_u P_-^{\perp}u, \partial_x \tilde{e}_u) - \sum_j (g''(u)\{\tilde{e}_u\}\{P_-^{\perp}u\}[\tilde{e}_u])_{j-\frac{1}{2}}, \\ \mu_5 = \dfrac{1}{2}(g''(u)(P_-^{\perp}u)^2, \partial_x \tilde{e}_u) + \dfrac{1}{2}\sum_j (g''(u)\{P_-^{\perp}u\}^2[\tilde{e}_u])_{j-\frac{1}{2}}, \\ \mu_6 = \dfrac{1}{6}(g_u'''(\tilde{e}_u - P_-^{\perp}u)^3, \partial_x \tilde{e}_u) + \dfrac{1}{6}\sum_j (\tilde{g}_u'''\{\tilde{e}_u - P_-^{\perp}u\}^3[\tilde{e}_u])_{j-\frac{1}{2}}. \end{cases} \tag{C3}$$

After integration by parts, we can easily get

$$\mu_1 = -\left(\partial_x(f'(u) - w), \frac{\tilde{e}_u^2}{2}\right) \leqslant c\|\tilde{e}_u\|^2. \tag{C4}$$

We rewrite μ_2 as

$$\mu_2 = -((g'(u) - g'(u_j))P_-^{\perp}u, \partial_x \tilde{e}_u) - (g'(u_j)P_-^{\perp}u, \partial_x \tilde{e}_u) - \sum_j (g'(u)\{P_-^{\perp}u\}[\tilde{e}_u])_{j-\frac{1}{2}}. \tag{C5}$$

By the definition of the projection, the second term of the equation is zero. And we also have $|g'(u) - g'(u_j)| = O(h), u_j = u(x_j)$ because $g''(u) = f''(u)$ is bounded. Then by the Cauchy-Shwartz inequality and Lemma 7, we have $|((g'(u) - g'(u_j))P_-^{\perp}u, \partial_x \tilde{e}_u)| \leqslant c\|P_-^{\perp}u\| \|\tilde{e}_u\| \leqslant ch^{2k+2} + c\|\tilde{e}_u\|^2$. For the third term, by Taylor's expansion,

$$g'(u) = g'(\{u_h\}) + g''\{e_u\}. \tag{C6}$$

Then, by the inequality (23), we have

$$|g'(u)| \leqslant \hat{a}(\hat{g}; u_h) + C\|e_u\|_\infty. \tag{C7}$$

Hence by Young's inequality and the boundedness of $\hat{a}(\hat{g}; u_h)$, we get

$$\sum_j (g'(u)\{P_-^\perp u\}[\tilde{e}_u])_{j-\frac{1}{2}} \leqslant \frac{1}{6}\sum_j (\hat{a}(\hat{g}; u_h)[\tilde{e}_u]^2)_{j-\frac{1}{2}} + Ch^{-1}\|e_u\|_\infty^2\|\tilde{e}_u\|^2 + ch^{2k+1}. \tag{C8}$$

Now, we can obtain the estimate of μ_2,

$$\mu_2 \leqslant \frac{1}{6}\sum_j (\hat{a}(\hat{g}; u_h)[\tilde{e}_u]^2)_{j-\frac{1}{2}} + (C + Ch^{-1}\|e_u\|_\infty^2)\|\tilde{e}_u\|^2 + ch^{2k+1}.$$

Next, we estimate μ_3. After integration by parts, we have

$$\mu_3 = -\frac{1}{6}((\partial_x(g''(u)), \tilde{e}_u^3) + \frac{1}{4}\sum_j (g''(u)[\tilde{e}_u]^3)_{j-\frac{1}{2}}).$$

By Taylor's expansion, the inequality (23), and Lemma 7, we have

$$\begin{aligned} g''(u)[\tilde{e}_u] &= (g''(\{u_h\}) - g'''\{e_u\})[\tilde{e}_u] \\ &= (g''(\{u_h\}) - g'''\{e_u\})([u_h] + [P_-^\perp u]) \\ &= g''(\{u_h\})([u_h] + [P_-^\perp u]) - g'''\{e_u\}([u_h] + [P_-^\perp u]) \\ &\leqslant 8\hat{a}(\hat{g}, u_h) + C[u_h]^2 + C|P_-^\perp u| + C|e_u|(|[u_h]| + |P_-^\perp u|) \\ &\leqslant 8\hat{a}(\hat{g}, u_h) + C(\|e_u\|_\infty^2 + \|P_-^\perp u\|_\infty + \|e_u\|_\infty^2 + \|e_u\|_\infty\|P_-^\perp u|\|_\infty) \\ &\leqslant 8\hat{a}(\hat{g}, u_h) + C(h + \|e_u\|_\infty^2). \end{aligned} \tag{C9}$$

Then, by Lemma 6, we have

$$\begin{aligned} \mu_3 &\leqslant C\|\tilde{e}_u\|_\infty\|\tilde{e}_u\|^2 + \frac{1}{3}\sum_j (\hat{a}(\hat{g}; u_h)[\tilde{e}_u]^2)_{j-\frac{1}{2}} + C(h + \|e_u\|_\infty^2)h^{-1}\|\tilde{e}_u\|^2 \\ &\leqslant \frac{1}{3}\sum_j (\hat{a}(\hat{g}; u_h)[\tilde{e}_u]^2)_{j-\frac{1}{2}} + (C + C\|\tilde{e}_u\|_\infty + Ch^{-1}\|e_u\|_\infty^2)\|\tilde{e}_u\|^2. \end{aligned} \tag{C10}$$

By Young's inequality, Lemmas 7 and 6, we have

$$\begin{cases} \mu_4 \leqslant Ch^{-1}\|P_-^\perp u\|_\infty\|\tilde{e}_u\|^2 \leqslant C\|\tilde{e}_u\|^2 \\ \mu_5 \leqslant Ch^{-1}\|P_-^\perp u\|_\infty\|P_-^\perp u\|\|\tilde{e}_u\| \leqslant C\|\tilde{e}_u\|^2 + Ch^{2k+2} \\ \mu_6 \leqslant C\|e_u\|_\infty^2(\|\tilde{e}_u\| + \|P_-^\perp u\|)h^{-1}\|\tilde{e}_u\| \leqslant Ch^{-1}\|e_u\|_\infty^2(\|\tilde{e}_u\|^2 + Ch^{2k+2}). \end{cases} \tag{C11}$$

Therefore, we complete the esitmate.

Conflict of Interest On behalf of all authors, the corresponding author states that there is no conflict of interest.

Funding This work was supported by the National Numerical Windtunnel Project NNW2019ZT4-B08, Science Challenge Project TZZT2019-A2.3, and the National Natural Science Foundation of China Grant no. 11871449.

References

1. Abramowitz, M., Stegun, I.A.: Handbook of Mathematical Functions: With Formulas, Graphs, and Mathematical Tables (National Bureau of Standards Applied Mathematics Series No. 55). U.S. Government Printing Office, Washington (1965)
2. Bona, J., Chen, H., Karakashian, O., Xing, Y.: Conservative, discontinuous Galerkin methods for the generalized Korteweg-de Vries equation. Math. Comput. **82**, 1401–1432 (2013)
3. Ciarlet, P.: The Finite Element Method for Elliptic Problem. North Holland, Amsterdam (1975)
4. Cockburn, B., Guzmán, J.: Error estimate for the Runge-Kutta discontinuous Galerkin method for transport equation with discontinuous initial data. SIAM J. Numer. Anal. **46**, 1364–1398 (2008)
5. Cockburn, B., Shu, C.-W.: TVB Runge-Kutta local projection discontinuous Galerkin finite element method for conservation laws II: general framework. Math. Comput. **52**, 411–435 (1989)
6. Cockburn, B., Shu, C.-W.: The Runge-Kutta discontinuous Galerkin method for conservation laws V: multidimensional systems. J. Comput. Phys. **141**, 199–224 (1998)
7. Cockburn, B., Lin, S.Y., Shu, C.-W.: TVB Runge-Kutta local projection discontinuous Galerkin finite element method for conservation laws III: one-dimensional systems. J. Comput. Phys. **84**, 90–113 (1989)
8. Cockburn, B., Hou, S., Shu, C.-W.: The Runge-Kutta local projection discontinuous Galerkin finite element method for conservation laws IV: the multidimensional case. Math. Comput. **54**, 545–581 (1990)
9. Cockburn, B., Luskin, M., Shu, C.-W., Süli, E.: Enhanced accuracy by post-processing for finite element methods for hyperbolic equations. Math. Comput. **72**, 577–606 (2003)
10. Di, Y.N., Li, R., Tang, T., Zhang, P.W.: Moving mesh finite element methods for the incompressible Navier-Stokes equations. SIAM J. Sci. Comput. **26**, 1036–1056 (2005)
11. Donea, J., Huerta, A., Ponthot, J.P., Rodríguez-Ferran, A.: Arbitrary Lagrangian-Eulerian methods. In: Stein, E., de Borst, R., Hughes, T.J.R. (eds.) Encyclopedia of Computational Mechanics, pp. 413–437. John Wiley & Sons, Ltd (2004)
12. Fornberg, B., Whitham, G.B.: A numerical and theoretical study of certain nonlinear wave phenomena. Philos. Trans. R. Soc. Lond. Ser. A Math. Phys. Sci. **289**, 373–404 (1978)
13. Fu, P., Schnücke, G., Xia, Y.: Arbitrary Lagrangian-Eulerian discontinuous Galerkin method for conservation laws on moving simplex meshes. Math. Comput. **88**, 2221–2255 (2019)
14. Gardner, C.S.: Korteweg-de Vries equation and generalizations. IV. The Korteweg-de Vries equation as a Hamiltonian system. J. Math. Phys. **12**, 1548–1551 (1971)
15. Goda, K.: On stability of some finite difference schemes for the Korteweg-de Vries equation. J. Phys. Soc. Jpn. **39**, 229–236 (1975)
16. Guillard, H., Farhat, C.: On the significance of the geometric conservation law for flow computations on moving meshes. Comput. Methods Appl. Mech. Eng. **190**, 1467–1482 (2000)
17. Hirt, C.W., Amsden, A.A., Cook, J.L.: An arbitrary Lagrangian-Eulerian computing method for all flow speeds. J. Comput. Phys. **14**, 227–253 (1974)
18. Hong, X., Xia, Y.: Arbitrary Lagrangian-Eulerian discontinuous Galerkin method for hyperbolic equations involving δ-singularities. SIAM J. Numer. Anal. **58**, 125–152 (2020)
19. Huang, W.Z., Ren, Y., Russell, R.D.: Moving mesh partial differential equations (MMPDEs) based upon the equidistribution principle. SIAM J. Numer. Anal. **31**, 709–730 (1994)
20. Huang, W.Z., Russell, R.D.: Adaptive Moving Mesh Methods. Springer, Berlin (2010)
21. Kalantari, I.: Induction over the continuum. In: Friend, M., Goethe, N.B., Harizanov, V.S. (eds.) Induction, Algorithmic Learning Theory, and Philosophy. Logic, Epistemology, and the Unity of Science, vol. 9, pp. 145–154. Springer, Dordrecht (2007)
22. Karakashian, O., Xing, Y.: A posteriori error estimates for conservative local discontinuous Galerkin methods for the generalized Korteweg-de Vries equation. Commun. Comput. Phys. **20**, 250–278 (2016)
23. Kennedy, C.A., Carpenter, M.H.: Additive Runge-Kutta schemes for convection-diffusion-reaction equations. Appl. Numer. Math. **44**, 139–181 (2003)

24. Klingenberg, C., Schnücke, G., Xia, Y.: Arbitrary Lagrangian-Eulerian discontinuous Galerkin method for conservation laws: analysis and application in one dimension. Math. Comput. **86**, 1203–1232 (2017)
25. Klingenberg, C., Schnücke, G., Xia, Y.: An arbitrary Lagrangian-Eulerian local discontinuous Galerkin method for Hamilton-Jacobi equations. J. Sci. Comput. **73**, 906–942 (2017)
26. Korteweg, D.J., de Vries, G.: On the change of form of long waves advancing in a rectangular canal, and on a new type of long stationary waves. Phil. Mag. **39**, 422–443 (1895)
27. Kutluay, S., Bahadir, A.R., Özdeş, A.: A small time solutions for the Korteweg-de Vries equation. Appl. Math. Comput. **107**, 203–210 (2000)
28. Li, R., Tang, T.: Moving mesh discontinuous Galerkin method for hyperbolic conservation laws. J. Sci. Comput. **27**, 347–363 (2006)
29. Liu, H., Yi, N.: A Hamiltonian preserving discontinuous Galerkin method for the generalized Korteweg-de Vries equation. J. Comput. Phys. **321**, 776–796 (2016)
30. Reed, W.H., Hill, T.R.: Triangular mesh methods for the Neutron transport equation, Los Alamos Scientific Laboratory Report LA-UR-73-479. Los Alamos, NM (1973)
31. Sun, Z., Xing, Y.: On structure-preserving discontinuous Galerkin methods for Hamiltonian partial differential equations: energy conservation and multi-symplecticity. J. Comput. Phys. 109662 (2020)
32. Tang, H.Z., Tang, T.: Adaptive mesh methods for one- and two-dimensional hyperbolic conservation laws. SIAM J. Numer. Anal. **41**, 487–515 (2003)
33. Vliegenthart, A.C.: On finite-difference methods for the Korteweg-de Vries equation. J. Eng. Math. **5**, 137–155 (1971)
34. Xia, Y., Xu, Y., Shu, C.-W.: Efficient time discretization for local discontinuous Galerkin methods. Discrete Contin. Dyn. Syst. Ser. B **8**, 677–693 (2007)
35. Xu, Y., Shu, C.-W.: Error estimates of the semi-discrete local discontinuous Galerkin method for nonlinear convection-diffusion and KdV equations. Comput. Methods Appl. Mech. Eng. **196**, 3805–3822 (2007)
36. Xu, Y., Shu, C.-W.: Local discontinuous Galerkin methods for high-order time-dependent partial differential equations. Commun. Comput. Phys. **7**, 1–46 (2010)
37. Xu, Y., Shu, C.-W.: Optimal error estimates of the semidiscrete local discontinuous Galerkin methods for high order wave equations. SIAM J. Numer. Anal. **50**, 79–104 (2012)
38. Yan, J., Shu, C.-W.: A local discontinuous Galerkin method for KdV type equations. SIAM J. Numer. Anal. **40**, 769–791 (2002)
39. Zhang, C., Xu, Y., Xia, Y.: Local discontinuous Garlerkin methods to a dispersive system of KdV-type equations. J. Sci. Comput. **86**, 4 (2021)
40. Zhang, Q., Shu, C.-W.: Error estimates to smooth solutions of Runge-Kutta discontinuous Galerkin methods for scalar conservation laws. SIAM J. Numer. Anal. **42**, 641–666 (2004)
41. Zhang, Q., Xia, Y.: Conservative and dissipative local discontinuous Galerkin methods for Korteweg-de Vries type equations. Commun. Comput. Phys. **25**, 532–563 (2019)
42. Zhou, L., Xia, Y., Shu, C.-W.: Stability analysis and error estimates of arbitrary Lagrangian-Eulerian discontinuous Galerkin method coupled with Runge-Kutta time-marching for linear conservation laws. ESAIM Math. Model. Num. Anal. **53**, 105–144 (2019)